Table 8.12. *Comparison of all-season PMP with May PMP (2 month offset) in the 973-mi² Auburn drainage (Sierra region).*

	Duration	1 hr	6 hr	12 hr	24 hr	48 hr	72 hr
1.	All-season basin (973-mi²) average depth (in.) PMP from Chapter 10, Table 10.1.	2.20	6.90	11.21	17.72	29.56	34.64
2a.	Average PMP index (10-mi², 24-hour) value (in.) from Plate 2 for the basin.				24.6		
2b.	All-season Sierra depth-duration ratios from Table 8.3.	0.14	0.42	0.65	1.00	1.56	1.76
3.	All-season 10-mi² average depth (in.) PMP for the basin (line 2a times line 2b).	3.4	10.3	16.0	24.6	38.4	43.3
4.	May index PMP as a ratio of all-season index PMP from Chapter 7, Figure 7.5.				.68		
5.	May average PMP index value (in.) for the basin (line 4 times line 2a).				16.7		
6.	May depth-duration ratios for 10 mi² from Table 8.5.	0.148	0.437	0.663	1.000	1.451	1.549
7.	May 10-mi² average depth (in.) PMP for the basin (line 6 times line 5).	2.5	7.3	11.1	16.7	24.2	25.9
8.	Depth-area reduction ratios interpolated for the basin (973-mi²) from Table 8.9.	0.548	0.607	0.648	0.687	0.731	0.773
9.	May basin (973-mi²) average depth (in.) PMP (line 7 times line 8).	1.4	4.4	7.2	11.5	17.7	20.0
10.	Ratios of May 10-mi² average depth PMP for the basin to the all-season 10-mi² average depth PMP for the basin (line 7 divided by line 3).	0.735	0.709	0.694	0.679	0.630	0.598
11.	Ratios of May basin (973-mi²) average depth PMP to the all-season basin (973-mi²) average depth PMP (line 9 divided by line 1).	0.636	0.638	0.642	0.649	0.599	0.577

Tahoe. The Auburn drainage is shown on the map in Chapter 10, Figure 10.1 The procedure begins by obtaining the all-season PMP from Chapter 10, Table 10.1 (line 1 of Table 8.12). The values on line 1 are not needed in the process used to get PMP for an off-season month, but are included in the table so they may be compared with the derived off-season PMP. Next, we obtain the basin-average PMP from the PMP Index map using any well-established technique (line 2a). Multiplying line 2a by the all-season, depth-duration ratios (line 2b) for the Sierra region from Table 8.3 results in line 3. Line 3 will be used only to derive line 10 for comparison with line 11 in comment "A." below. Then Chapter 7, Figure 7.5 is used to get the average percentage value in the drainage for May (line 4). Multiplication of line 3 at 24 hours and line 4 provides us with the index value of PMP for May (line 5). Lines 6 and 8 contain the seasonally-adjusted DAD. Examination of Figures 7.2 through 7.11 reveals that the all-season envelope of months at Auburn runs from November through March. Thus May becomes a 2-month offset. The line 6 values are read directly from Table 8.5. Any reasonable interpolation scheme of the values in Table 8.9 may be used to get the values on line 8. The procedures followed in lines 2 through 10 would be used to obtain off-season PMP for any drainage.

As for the ratios on line 11 of Table 8.12, one should expect these values to reflect the peculiar circumstances of the drainage in question and the month under consideration. In the case illustrated here, *viz.* Auburn in May, it is of significance to note that:

A. Comparing lines 10 and 11, notice that for all durations, the reduction in PMP potential in May (spring) as compared with the all-season months - October through March (winter) - is greater at 973 mi^2 than at 10 mi^2. This would seem to indicate that there is a greater decrease in the capacity of the atmosphere to produce widespread, orographic precipitation in the spring, *vis a vis* winter, than in the atmosphere's capacity to produce smaller scale, intense precipitation during the same seasonal interval, at least in the Sierra of California.

B. The results in line 11 show that when the May basin average depth of PMP (line 9) is compared to the all-season (winter) basin average depth of PMP (line 1), the reduction potential in May is greater at 2 and 3 days than at 1 day. This reflects a lesser capacity of the atmosphere to produce consecutive (or

repeating) heavy precipitation episodes in the Spring in the California Sierra, *vis a vis* the winter.

C. Furthermore, why is the reduction in PMP potential in line 11 at 1 hour greater than at 6, 12, and 24 hours? Perhaps the answer lies in reframing the question to ask why the ratios at 6, 12, and 24 hours are greater than at 1 hour. We are not certain of the answer, but it can be speculated that in the durational range of 6 to 24 hours, atmospheric conditions in some manner in the spring are more favorable to synergistic interactions among the small-scale, heavy precipitation-producing elements than in the winter; while, at the same time, 1 hour is not sufficient time for such (speculative) interactions to take place regardless of season. Hence, there is a relative percentage increase at 6 through 24 hours, compared with the 1-hour percentage.

9. LOCAL-STORM PMP

9.1 Introduction

Local-storm probable maximum precipitation (PMP) estimates were developed to provide rainfall values for small basins and short-duration storms in California. HMR 49 (1977) was the first report to provide such estimates for the state. HMR 49 excluded the northwestern corner of California (see Figure 4.1 in HMR 49 for exact area) from local-storm PMP consideration. It was believed that the stable Pacific air usually predominating in this region precluded the development of excessive thunderstorm rainfall. However, the revised PMP for the northwestern United States, HMR 57 (1994) provides PMP estimates west of the Cascade mountain divide to the coast. In order to maintain continuity with HMR 57 the current study extends PMP to the northwest coast of California. This was done despite the fact that no major new storms were observed in that area since the publication of HMR 49. HMR 49 used data for the period from 1940-1972; an additional 25 years were available for the current study.

9.2 Definition and Methodology

The definition of local storms in the PMP process has remained relatively constant since the term was first applied in HMR 43 (1966), but the changes that were made are important. As defined in HMR 49 they are "unusually heavy rains exceeding 3 inches in 3 hours or less that are reasonably isolated from surrounding rains." The maximum duration allowed for such storms was increased to 6 hours in HMR 49 to account for the merging of several shorter duration events. In HMR 49 the areal coverage was defined for storms ranging up to a maximum of 500 mi^2, although the majority of storms cover an area substantially less than this. One of the biggest problems in defining local storms is the issue of "reasonably isolated" rainfall. Many times significant storms are embedded within a more widespread light or moderate rainfall pattern, and it is a matter of some debate as to which storms of this type to include. Several embedded locally heavy rains in California storms have been included in the list of record local storms, shown in Table 9.1. HMR 49 restricted such embedded storm types to the warm season, from about May through October. However,

Table 9.1. *Extreme local storms in California (rainfall in inches, duration in minutes).*

#	Location	Lat. Lon.	Elev	Date	Rainfall	Duration	References
1.	Encinitas	32°59' -117°15'	100	10/12/1889	7.58	8 hours	Pyke 1975
2.	Campo	32°36' -116°28'	2590	8/12/1891	11.5	80	HMR 37
3.	Kennett	40°45' -122°24'	730	5/9/1915	8.25	8 hours	HMR 37
4.	Wrights	37°08' -121°55'	1600	9/12/1918	3.5	60	HMR 37
5.	Red Bluff	40°09' -122°15'	340	9/14/1918	4.7	180	HMR 37
6.	Campo	32°36' -116°28'	2590	7/18/1922	7.1	120	CD 1922
7.	Squirrel Inn	34°14' -118°15'	5280	7/18/1922	5.01	90	CD 1922
8.	Tehachapi	35°08' -118°27'	3975	9/30/1932	10.6	5 hours	USCOE 1961; HMR 50
9.	Indio	33°43' -116°13'	-12	9/24/1939	6.75	6 hours	Pyke 1975
10.	Fullerton Creek	33°54' -117°55'	400	3/14/1941	2.51	40	USCOE 1941a.
11.	Needles	34°51' -114°36'	480	8/9/1941	2.00	60	USCOE 1941b.
12.	Avalon	33°21' -118°19'	10	10/21/1941	5.53	210	HMR 37
13	Los Angeles	34°00' -118°10'	500	3/3/1943	3.32	180	HMR 37
14.	Tehachapi	35°08' -118°27'	3975	10/6/1945	3.17	120	HMR 49
15.	Cucamonga	34°05' -117°25'	1650	9/29/1946	3.20	80	San Bernardino FCD
16.	La Quinta	33°40' -116°19'	50	7/22/1948	3.00	210	USCOE 1957
17.	Fresno (NE of)	37°09' -119°30'	1100	5/17/1949	2.26	60	USWB 1949
18.	Vallecito	32°58' -116°21'	1450	7/18/1955	7.1	70	USCOE 1955
19.	Chiatovich Flat	37°44' -118°15'	10320	7/19/1955	8.25	150	Kesseli & Beaty 1959
20.	Santa Barbara	34°26' -119°43'	10	2/4/1958	1.66	70	USCOE 1958
21.	Newton	40°42' -122°22'	700	9/18/1959	10.6	5 hours	HMR 37
22.	Darwin	36°16' -117°35'	4900	7/13/1967	3.35	20	Cal. DWR 1973
23.	Los Angeles	34°00' -118°10'	270	11/19/1967	1.51	30	CD 1967
24.	Bakersfield	35°25' -119°03'	475	6/7/1972	3.00	60	Bryant 1972
25.	Redding	40°34' -122°25'	580	8/14/1976	3.20	240	Fontana 1977
26.	Borrego	33°12' -116°20'	576	9/23/1976	4.00	180	USCOE 1977
27.	Goleta	34°26' -119°53'	10	10/1/1976	4.00	90	Santa Barbara FCD 1976
28.	Santa Barbara	34°25' -119°42'	100	1/10/1978	1.37	20	Santa Barbara FCD 1978
29.	Forni Ridge	38°48' -120°13'	7600	6/18/1982	5.76	6 hours	Kuehn 1983
30.	Palomar Mtn.	33°21' -116°52'	5550	8/13/1992	6.40	120	HPD 1992
31.	Copco	41°59' -122°21'	3000	7/21/1995	2.30	30	NWS 1995

the current study showed that some important local storms of the *embedded type* occurred in the cool season and are included here. As will be seen in this report, the former distinction between general- and local-storms has been blurred and a more complex array of storm types is recognized.

Local-storm PMP followed a methodology first used in the studies for the northwest United States, in HMR 43, HMR 49, HMR 55A (1988) and later in HMR 57.

9.3 Storm Record

The first and perhaps most important step in PMP development is the selection of the major local storms that will form the cornerstone for the calculation of PMP. One starting point was the list of major short-period rains contained in the PMP study for the Colorado River and Great Basin, HMR 49. The California major local storms, including those from HMR 49, are listed in chronological order in Table 9.1. The locations of the 31 storms are shown in Figure 9.1. Some minor corrections for latitude and longitude errors in the HMR 49 list were made, as well as the addition of 14 new storms. Seven of the *new* storms in Table 9.1 predate the 1975 data cutoff in HMR 49, but were not included in the HMR 49 list for a number of reasons. Either they had been overlooked completely, were examined and rejected due their *hybrid* nature, or did not quite meet the rainfall intensity criteria established in HMR 49. As a result of revised criteria and re-examination, seven storms which occurred prior to 1975 were added: 9. Indio, September 24,1939; 10. Fullerton, March 14, 1941; 11. Needles, August 9,1941; 17. Fresno, May 17, 1949; Santa Barbara, February 4, 1958; 22. Darwin, July 13, 1967; and 23. Los Angeles, November 19, 1967. The number are for reference in locating the storms on the map in Figure 9.1. Seven extreme local storms which occurred since the publication of HMR 49 were also added. The seven new storms include: 25. Redding, (Aug.14, 1976); 26. Borrego, (Sept.23, 1976); 27. Goleta, (Nov.1, 1976); 28. Santa Barbara, (Jan.10, 1978); 29. Forni Ridge, (June 18, 1982); 30. Palomar Mountain, (Aug.8, 1992); and 31. Copco, (July 21, 1995). Three of the most important new storms: Redding, Forni Ridge and Palomar Mountain, are discussed in detail later in this chapter.

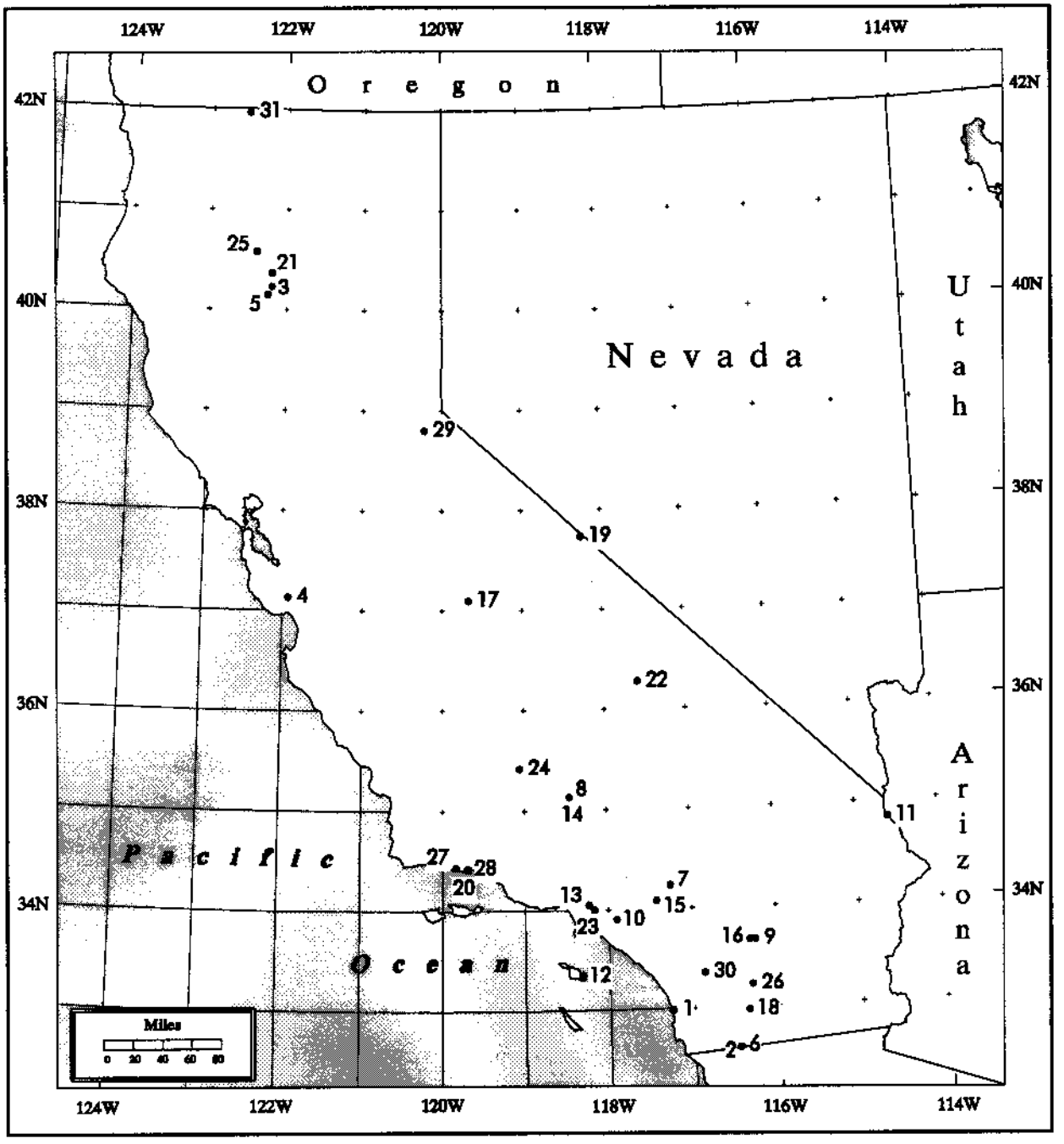

Figure 9.1. *Location of major local storms of record. The numbers refer to the list of storms found in Table 9.1.*

Several sources may be consulted for more information on the earlier storms listed in Table 9.1. HMR 37 (1962) contains detailed discussions on many of the storms which occurred up through 1960. HMR 50 (1981) also includes summaries of other major storms found in Table 9.1. Many of these storms have varied documentation; the references in Table 9.1 are to either original data sources or to the most comprehensive study which this office could locate. In cases where information is not available in the general literature, readers interested in complete documentation of a particular storm can contact the Hydrometeorological Design Studies Center where files on the storms are currently maintained.

In order to establish depth-duration and depth-area relations with a larger number of storms, a second list of local storms was also prepared. These storms did not generally meet the most extreme criteria, but were important nonetheless. They are listed in Appendix 3, Table A3.1 and consist of 137 storms from the National Weather Service Cooperative Station network. These storms cover the period from 1948-1992 and are considered very reliable in terms of depth and time measurements. The data were extracted from the National Climatic Data Center's (NCDC) Hourly Precipitation Data tapes. The relative sparseness of this network is illustrated by the fact that there is only one station for every 650 mi^2 in California. This presents a particular problem in the analysis of local storms, which by definition cover an area of 500 mi^2 or less, usually a much smaller area.

9.4 Meteorology of California Local Storms

The large-scale features that control the development and type of extreme storms affecting California are well-known, and are documented in HMR 37 and HMR 50. At the planetary scale, four or five Rossby waves are the most common flow configuration in the northern hemisphere, and both modes favor a long-wave ridge position over western United States. This *ridging* dampens the intensity of systems moving into the long-wave ridge. Of course large-scale troughs do develop and can help to intensify short-wave disturbances moving through them. An interesting and important exception to the *normal* flow pattern over the west occurs during El Niño events. The El Niño often causes a split flow in the westerlies and brings anomalously wet weather to much of southern California.

The climate of the western United States is also strongly influenced by large subtropical high pressure zones: the Bermuda High and the Pacific High. Subsidence along the east side of the Pacific High frequently affects western United States, bringing stable atmospheric conditions to coastal regions. Northwest flow also produces upwelling in the coastal water which further cools the lower levels of the atmosphere and enhances stability, thus producing a marine stratus layer and frequent coastal fog. This stable coastal air partially explains the relative lack of thunderstorm activity along the California coast (Changery 1981). Even though the Bermuda High is thousands of miles east of California, it also plays a role in the regional climate, as moist, unstable air along its western periphery can be pulled into the Southwest This pattern, often referred to as the Southwest summer monsoon, occurs most frequently from June through August. Recent research has increased understanding of the Southwest monsoon structure and of moisture sources for heavy rainfall in western United States (Carleton 1985, Douglas 1995), as will be discussed in the section on moisture, 9.5 of this chapter.

Local storm development is influenced to a large degree by the synoptic-scale patterns operating over California. As noted above, subsidence beneath the Pacific High is a frequent occurrence, and short waves moving into a ridge position are usually dampened, reducing the potential for strong storms. Significant troughs are often restricted to northern California and the cool season, which reduce the likelihood of strong convective activity. Several other synoptic features, however, can act to enhance local-storm potential. The so-called *thermal low* caused by intense summertime heating over the desert areas, produces an inverted trough that can reach from Mexico to Canada. This trough, enhanced by downslope warming from the mountains adjacent to the desert, can play a role in the initiation of convection, as will be seen in one of the case studies.

California terrain plays a critical role in determining frequency, location, and intensity of local storms in the state. The major features are well-known. A narrow coastal zone and long chain of north-south oriented coastal ranges block the inflow of Pacific moisture except at a few locations. A broad, flat interior valley, the Central Valley is bordered on the east by the massive Sierra Nevada mountains, on the north by the southern end of the Cascade range, and on the south by the Tehachapi mountains which separate divide the Central Valley from the deserts of southeast California. The terrain is somewhat more complex in southern California where the San Gabriels and San Bernardinos run west to east from Santa Barbara,

with more mountains extending south to the Mexican border. The only appreciable coastal plain in the south is the Los Angeles basin. The unique terrain of California has a strong impact on mesoscale and local-scale meteorological phenomena, and will be discussed at various points in this chapter.

Extreme local storms in California are usually convective storms, although not always of a classical, isolated thunderstorm type. Mesoscale convective features such as squall lines are sometimes embedded within cool season larger scale synoptic storms. Embedded local storms also result from eastern Pacific tropical cyclones which occasionally affect California. Some of the most intense short-duration rainfalls have occurred when a tropical cyclone or its remnant moisture has moved into California. One of the best recent examples was when the remnants of Tropical Storm Kathleen moved across southern California September 9-11, 1976. Widespread heavy rainfall fell across southern California from this storm, as well as intense short-duration rainfall, such as 4.8 inches in 3 hours at Mt. Laguna, San Diego County. This storm is not listed in Table 9.1, although a more localized event at Borrego on September 23, 1976 is included. The latter storm was the result of a tropical air incursion that resulted in very heavy rains. Although relatively rare, tropical disturbances can and do enter southern California and produce significant rainfall. The only tropical storm intense rainfall known to have entered central or northern California, although the center remained offshore, occurred during September 1918 and this storm produced two of the storms in Table 9.1, Wrights and Red Bluff. HMR 37 provides a detailed explanation of the meteorological aspects of this unique storm.

The so called *true* local storm is typically a very isolated thunderstorm, which develops without the strong, large-scale lifting mechanisms that produce widespread rainfall. These local storms can dump copious rainfall over a very small area, with little significant precipitation even a short distance away. The greatest recorded local storm in California history occurred on August 12, 1891 at Campo (Storm 6 in Fig. 9.1), where 11.50 inches fell in 80 minutes. Evidence gathered at the time of this storm indicates that this storm was very limited in area, although supporting information is scanty (HMR 50). The small scale of local storms means that they are very often missed by the conventional rain gage network. It is hoped that the advent of new observing systems, such as the WSR-88D radar and the Automated Surface Observing System (ASOS) will increase the likelihood of *catching* these local storms. In California they usually occur during the warm season, from April to

October, when moisture and solar energy are closer to their annual maxima. Another type of storm which has been less frequently recognized as affecting California is Mesoscale Convective Systems (MCSs). Each of these storm types: embedded storms, isolated thunderstorms, and MCSs will be discussed below with one or more examples to illustrate aspects of the various storm types.

In Section 9.5, which deals with maximum dewpoints, the discussion focuses on the spatial and temporal evolution of moisture fields across the state. In the current section (9.4) some of the dynamics of extreme storms which affect the state are examined. This will be important later in considering the question of transposing storms.

As stated earlier, several different storm types can produce extreme local storms in California. One of the seminal works on flash floods in the western United States (Maddox et al. 1980) showed that in California, the most common example is strong synoptic systems, or Type III. In this study, 8 out of 10 California flash flood events were Type III storms. All the Type III storms occurred during the cool-season months. These flash flood events are clear-cut cases of an embedded local storm. Rainfall rates can be quite intense in embedded storms, although not usually as intense as in more isolated storms. Among the reasons for this are: embedded type storms are cool-season phenomena and have lower moisture content; and the widespread nature of the rainfall means that several storms may be competing for a finite amount of water vapor. On the other hand, the precipitation in such storms is often organized into mesoscale rainbands and transient wave features that act to enhance rain rates. The combined effect of merging rainbands and transient waves produced hourly rainfall rates of 1.6 to 1.7 inches per hour over western Los Angeles County during the morning of February 10, 1978 (not listed). Several of the storms in Table 9.1 belong to this type of strong synoptic system with embedded convection, including the Los Angeles storm of November 19, 1967 and the Santa Barbara storm of January 10, 1978.

As noted earlier, another storm type which can produce very heavy rainfall is the MCS. Comparatively little research has been done on the existence or behavior of MCSs in California. However, recent research drawn from the Southwest Area Monsoon Project (SWAMP) (Meitin et al. 1991) has confirmed that MCSs occur in Arizona and it is very likely that they can and do migrate into southeastern California. The term MCS refers to any precipitation system with a spatial scale of 20-500 km that includes deep convection during

part of its life cycle (Zipser 1982). Confirmation of the existence of MCSs was only made possible by the advent of geostationary satellites, so they are a relatively *new* phenomenon, at least in terms of research.

Fleming and Spayd (1986) studied very heavy convective rainfall events (≥2 inches) in western United States and classified the storms according to various meteorological and satellite characteristics. From 1981-1983, 9 such events occurred in California, 6 of which were considered MCS-type systems. Two were synoptic-scale, overrunning events, and one was classified as a single-cluster convective storm, i.e., a *true* local storm. The California MCS systems were all smaller (area and duration) than the Mesoscale Convective Complexes (MCCs) in the central United States, and smaller than the MCS-alpha systems found over other parts of western United States The California MCSs were of two types; MCS-beta circular and MCS-beta linear storms, with length scales of 50 to 150 km (30-100 miles). The MCS-beta circular storms develop in environments of little or no vertical wind shear and appear as round or oval in satellite imagery. MCS-beta linear systems occur in environments with strong vertical wind shear and appear as wedge-, carrot- or diamond- shaped in satellite imagery. All the MCS systems in California were confined to either the elevated terrain east of Los Angeles and San Diego or the deserts of the southeast. It is interesting to note that the Lytle Creek Foothill Boulevard storm of August 17, 1983 (2.65 inches in 1 hour), one of the largest storms from the NCDC list in Appendix 3, Table A3.1, was classified in the Fleming and Spayd (1986) study as an MCS-beta circular system. The storm resulted in severe highway flooding and several fatalities. The Palomar Mountain storm of August 13, 1992 was also an MCS-beta circular system.

The full-blown mesoscale convective complex (MCC), which must fulfill certain size, duration and cloud-top temperature requirements to be classified as such, seems to be very rare in California (Maddox 1983). Very few full-blown MCCs have been documented anywhere in the western United States, but a relatively recent storm on August 10, 1981 did meet the criteria (Randerson 1986). The storm, centered near Ute, Nevada, about 30 miles northeast of Las Vegas, Nevada, affected a very wide area, but the very intense rainfall of more than 6 inches in several hours, occurred over a much smaller area. In terms of intensity and depth-area-duration characteristics, this storm can easily be classified as local, although the rainfall was not completely isolated. The proximity of this storm to the California border (the Ute storm center was approximately 75 miles northeast of the state border) makes it an

important addition to the catalog of significant local storms. The occurrence of this storm suggests the likelihood that even large MCSs or possibly even MCCs can affect the deserts of the Southwest and possibly California. The depth-area characteristics of the Ute storm are discussed in greater detail in the depth-area section of this chapter (Section 9.9).

Many of the storms listed in Table 9.1 have been discussed in detail in HMR 50 and in other sources and this information is not repeated in this report. Meteorological discussions of three important recent storms are provided in the following sections to give the reader some insight into the variety of processes and factors that lead to extreme local rainfall in California..

9.4.1 Redding - August 14, 1976

Heavy rainfall in and around Redding on the afternoon of August 14, 1976 provides one of the best examples of a strong synoptic system occurring in the summer season. The upper-air pattern is similar to the Type III flash flood-producing storm type cited earlier (Maddox et al. 1980). The Redding storm also illustrates some of the reasons for such a pronounced PMP maximum in the northern end of the Central Valley and surrounding foothills (see Figure 9.23).

The following description and analysis of the Redding storm draws heavily on a paper by Fontana (1977) who studied the storm in detail. According to surveys conducted after the storm by the United States Army Corps of Engineers, the maximum precipitation was 8.8 inches in a 24-hour period ending on the morning of August 15, although most of the rain fell in a five-hour period on the evening of August 14. The maximum-intensity report included a 2.5-inch amount in one hour on the evening of the 14th. Several other stations received over 3 inches in a three-hour period the same evening. The heaviest precipitation, an area of 8+ inches, fell in the higher terrain just west of downtown Redding, while the NWS cooperative station (Redding 5 SSE) southeast of town recorded less than one inch (0.85 inches) during the same time period.

The strong synoptic pattern within which this storm developed is far more typical of winter than summer. In this case, an unusually vigorous mid-level shortwave moved into the long-wave trough position located just off the Oregon-California border. Evidence for the

existence and movement of the short wave is given by the area of strong geopotential height decreases of over 120 meters, at the 500-mb level during the 24-hour period preceding the storm from 12 UTC on August 13 to 12 UTC on August 14. Intensification of a shortwave generally leads to increased divergence aloft and increased vertical motion. In addition, a strong wind maximum on the west side of the upper trough indicated that the system was undergoing intensification or continued deepening during this same period.

The strong dynamics aloft led to significant changes at the surface which also served to enhance the rainfall in the Redding area. Early on the morning of August 14 a cold front moved south, reaching a line from the San Francisco Bay area to just south of Sacramento. Over the course of the day, the front began to retreat north as a warm front and approached the Redding area during the afternoon. At the same time, a surface trough, a reflection of the shortwave aloft, developed along the Oregon coast and began a southeastward movement. By 00 UTC on August 15, frontogenesis took place along the trough line, and a weak low-pressure circulation developed along the front to the northwest of Redding. The newly developed cold front and the northward-moving warm front merged very close to Redding forming an instant occlusion or triple point low. As pointed out by Junker (1992), intersecting boundaries provide an area of maximized low-level convergence and enhance the potential for convective development. The location and movement of the short-wave trough is also confirmed by a surface isallobaric analysis, which showed sharply falling pressures in northern California where the frontal wave developed. These falling pressures are indicative of upper level divergence, which is expected ahead of the short-wave trough.

Radar analysis of the storm from the Medford, Oregon and Sacramento radar sites confirms the basic sequence of events outlined above. In the hour from 2230 UTC to 2330 UTC, there was an explosive increase in convective activity close to where the fronts intersected and the surface wave was forming. The strongest radar echoes occurred from 0030 UTC to 0330 UTC on August 15, with one cell west of Redding showing a VIP (video integrator and processor) intensity of 5. This intensity level (2.0 to 5.0 inches per hour) corresponds well with the observed rainfall intensities found in the Corps survey after the storm.

In looking at extreme precipitation events, very high moisture is usually a critical component in leading to the event. In the Redding storm, however, this was not one of the

major factors. As seen in Figure 9.11, the 3-hour maximum persisting dewpoint (at 1000-mb) for the northern end of the Sacramento Valley is close to 73°F. Dewpoint readings at Red Bluff and stations to the south (from which the inflow was occurring on the day of the storm) were in the upper 50's to low 60's most of the day. While these readings are well above average (mean August dewpoints range from the mid-40's to low 50's in the upper Sacramento Valley area), they do not come close to the maximum levels possible in the area. Although obviously adequate to support heavy precipitation, the relatively low moisture levels in this event imply that a significant increase in rainfall would be likely, given the same dynamics combined with higher moisture. The theoretical moisture maximization for the storm was 1.82, based on a storm dewpoint of 61°F and a maximum persisting dewpoint of 73°F. The actual in-place maximization was restricted to 1.50 in keeping with local-storm procedures outlined in Section 9.5.2. This limitation does indicate a level of conservatism in the PMP process which is not always recognized.

9.4.2 Forni Ridge - June 18, 1982

For a dramatic example of an isolated extreme local-storm, Forni Ridge provides one of the best recent cases in California. The storm on the afternoon of June 18, 1982 occurred within the headwaters of the South Fork of the American River (#29 in Figure 9.1) between the communities of Kyburz and Strawberry (Kuehn 1983). The six-hour rainfall total of 5.76 inches is intense, but the shorter duration amounts were extraordinary: 1.50 inches in 5 minutes; 2.20 in 10; 2.80 in 15; 4.02 in 30; and 4.42 in one hour. The rain was recorded in a United States Bureau of Reclamation tipping-bucket gage, allowing for the temporal resolution to be described accurately. As pointed out by Kuehn (1983) the short-duration rainfall actually **exceeded** PMP as given in HMR 49; the 15-minute PMP was 2.69 inches, 0.11 inches **less** than the 2.80 that fell in 15 minutes at Forni Ridge. The degree of exceedance was even greater at durations below 15 minutes. There was tremendous runoff from this storm, owing to both the intensity of the storm and the fact that much of the vegetation in the area had been burned off in a wildfire the previous summer. According to Kuehn (1983), the discharge magnitude was one of the highest ever recorded in California for that basin size.

Another important aspect of the Forni Ridge storm is the high elevation at which it occurred, approximately 7600 feet. This is well above the elevation at which PMP begins

to decrease in both HMR 49 and in this report. Using the formula in HMR 49 (see Section 4.3.2 for details) a 13-percent reduction in the PMP index level would be expected for a storm at this elevation. Using a slightly different formula than in HMR 49, the current report (Section 9.7 - Elevation) would allow a percentage reduction of 14 percent for a basin at an elevation at 7600 feet. The occurrence of this storm at such an elevation is strong confirmation of the ability of the atmosphere to produce very heavy rainfall at levels well above levels at which the reduction in moisture was formerly believed to diminish storm amounts.

The meteorological factors leading to the Forni Ridge deluge included unusually high moisture at the surface and aloft as well, a strong upper-level trough, and an extension of the summertime thermal trough well north of its usual position.

Surface dewpoints at the closest observing stations to the storm site reflect the high moisture available for storm inflow. Blue Canyon, the nearest observing station (approximately 40 miles north-northwest of Forni Ridge) experienced a dramatic influx of moisture late on June 17 and early June 18, as dewpoints surged from the low 40's to low 50's (°F). When reduced to a common reference level of 1000 mb, Blue Canyon recorded a 3-hour maximum persisting dewpoint of 66°F, only about five degrees less than the maximum persisting values for mid-June shown in Figure 9.9. At Reno, 55 miles northeast of the storm site, the readings were only slightly less extreme, reaching a 3-hour maximum persisting value of 64°F at 1000-mb (maximum persisting of 72°F - see Figure 9.9). At 12-hours, the persistence of high moisture was even more striking at these stations, coming within one degree of the maximum persisting 12-hour value. Extremely high moisture was also observed at Red Bluff, located in the northern end of the Sacramento Valley. The moisture surged into Red Bluff late on the 17th, as the dewpoint jumped 16°F in one hour from 48°F to 64°F. High dewpoints were maintained throughout the 18th, with a maximum 3-hour value of 65°F (at 1000-mb), versus the extreme of 71°F. It is highly likely that these high dewpoints also affected Forni Ridge on the afternoon of June 18th, providing abundant moisture for heavy rainfall.

This extremely high moisture was due to a combination of factors. First, the interaction between the thermal trough which extended north into southern Canada and the Pacific high, created an onshore pressure gradient between these two features, allowing some

inland penetration of marine air. Furthermore, this air was intensely heated by the strong June sun, raising temperatures to 108°F at Red Bluff on June 17. In addition, as noted by Hill (1993) when the signature of a thermal trough extends up to 850 mb or higher (as it did on June 17-18, 1982), the circulation pattern draws subtropical moisture northward. At upper levels of the atmosphere a split-flow pattern existed across the state, with a highly amplified ridge extending from California all the way to northern British Columbia. A trough associated with the subtropical jet stream existed well to the south over Baja California. The central Sierra were in a (*col-like*) area between these two features. Winds aloft were quite weak, generally 10 to 15 knots at 500 mb and 20 to 25 knots at 300 mb. This upper-level weak flow slowed the movement of any thunderstorms that did form. Causes for convection on the scale of the Forni Ridge storm are often unresolvable on synoptic-scale maps, and there was not any strong synoptic feature, such as a short wave, to which this storm can be attributed. The complex terrain of the Sierra Nevada creates differential heating and cooling of slopes with resultant thermal circulations. In the daytime, upslope winds create areas of moisture convergence, which can lead to convective cloud formation and thunderstorms. The thermal trough itself is also known to initiate convection, as convergence into it forces lifting of air parcels. Instability was also clearly enhanced by the strong solar insolation on the day of the storm. Any of these factors could have led to the development of convective activity on a limited scale, but with very high moisture to draw on, an extremely unusual event unfolded.

9.4.3 Palomar Mountain - August 13, 1992

The storm at Palomar Mountain Observatory was one of the rare instances where extremely heavy rainfall was recorded in an NWS cooperative network rain gage. A two-hour storm total rainfall of 6.40 inches fell at this site on the afternoon of August 13, 1992. In the first hour of the storm, from 12:15 to 1:15 local standard time (2015 UTC to 2115 UTC), 4.70 inches fell. This was an amount far in excess of the 100-year return frequency amount of 1.80 inches. The two-hour amount at Palomar is very close to 50 percent of the two-hour PMP for this location. An isohyetal map of the Palomar storm is shown in Figure 9.2. Of interest as well is the rainfall center at Mt. Laguna, where 4.70 inches fell in less than four hours during about the same time period as the Palomar rainfall. The existence of two intense rainfall centers occurring so far apart (approximately 40 miles), but taking place almost concurrently indicates that there was more

than one thunderstorm involved in the storm system. This suggests that the storm is properly classified as an MCS, and satellite imagery confirms it as an MCS-beta circular type.

Palomar Mountain Observatory is located at 33° 21' N, 116° 52' W, at an elevation of 5548 feet. Although Palomar Mountain is one of the higher points in the local area, the terrain is quite mountainous, especially to the east. The mountain ranges of southern California, east of the San Diego metropolitan area, extend north-south in a nearly unbroken chain, separating the coastal plain from the interior deserts of the southeastern part of the state. As shown in the isohyetal map, heavy rainfall was confined to the higher terrain, with much lower amounts in the coastal plain and in the deserts just to the east.

The hemispheric flow pattern prior to the Palomar storm featured a meridional pattern, with an unusually amplified ridge at upper levels over the western United States, especially for August. Geopotential heights at 500-mb in this ridge centered over Nevada, reached a maximum of 5940 meters on the morning of August 13, and built somewhat more during the day. The ridge was so amplified that easterly flow had developed underneath the ridge from central Texas to southern California. This easterly flow provided one of the important ingredients toward the eventual development of the Palomar storm. The easterly flow helped to advect large amounts of mid-level moisture from southern Arizona into the mountains where the storms developed. In addition, the flow aloft remained rather weak throughout the day; at 700 mb ranging from light and variable to 10 knots. At 500 mb winds were easterly at only 5 knots on the morning of the 13th. Even at 200 mb winds were only 10 to 15 knots. The weakness of the flow contributed to the slow movement of the MCS and allowed the storm to take on the characteristic shape of an MCS circular system.

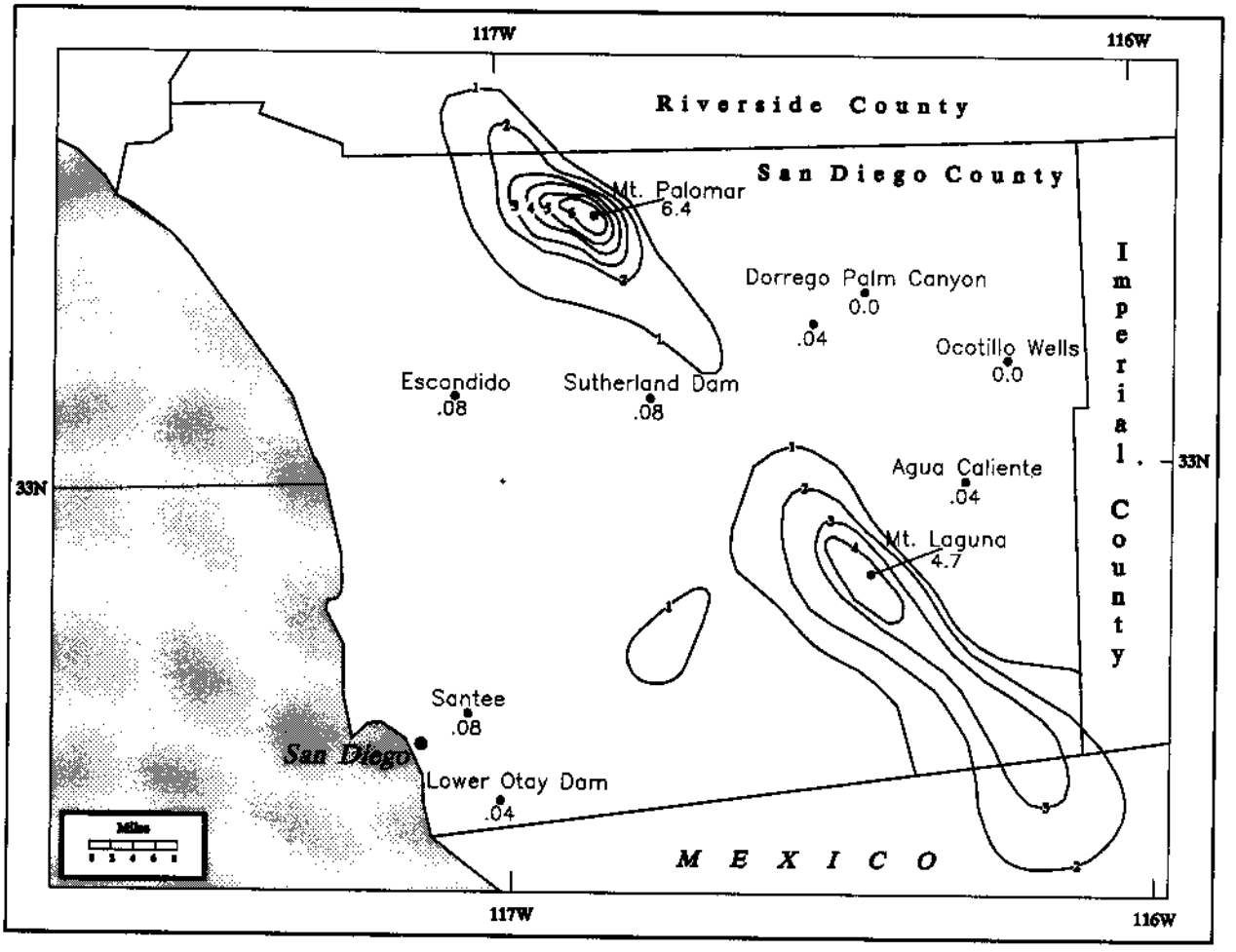

Figure 9.2. *Isohyets and recorded amounts, in inches, from the Palomar Mountain storm of August 13, 1992.*

Despite warm temperatures at the 500-mb level, ranging from -5 to -7°C over southern California and Arizona, convection was widespread indicating that there was no cap to inhibit convective development.

At the surface, a thermal trough (also referred to as a *heat low*) was located from Baja, California northward to the central part of the state, a more or less semipermanent feature in this area during the summer months. Circulation patterns associated with a strongly-developed (i.e., through a thick layer of the atmosphere) thermal trough can be conducive to drawing subtropical moisture northward into the eastern side of the trough (Hill 1993). In addition, convergence in the trough is often an aid in thunderstorm initiation, and may have played a role in the development of thunderstorms which affected southern and southeastern California over the three-day period, August 12-14, 1992. Surface temperatures well in excess of 100°F were recorded from the California desert areas northward to the Central Valley each day during this period, providing plenty of destabilizing energy to the lower atmosphere.

Low-level moisture was also extremely high in the period leading up to the Palomar storm. Surface dewpoints were well into the 70s across southern California; at Imperial, California dewpoints reached 79°F and 80°F at 1500 UTC and 1800 UTC on the 13th. These reading are at the extreme upper limit of moisture believed possible in southern California in August as shown in Figure 9.11. San Diego recorded a dewpoint of 70°F at 1500 UTC and 1800 UTC, just several hours prior to the onset of precipitation both there and at Palomar. The maximum three-hour persisting dewpoint for August at San Diego is 73°F. Precipitable water was also well above normal; at 1200 UTC (0500 PDT) on August 13 Miramar NAS, near San Diego, measured 1.64 inches or 164% of normal for the date. By the afternoon, 0000 UTC (1700 PDT) August 14, it had increased to 1.89 inches or 188% percent of normal (1700 PDT). This extremely high moisture had tropical origins in the Gulf of California and is visible on sequences of satellite water-vapor images for the day.

Scofield and Robinson (1992) have demonstrated the relationship between heavy convective rainfall and tropical water-vapor plumes. The plumes are tongues or streams of moisture, detectable on water-vapor imagery at 6.7 microns, and can indicate high moisture between the 700- and 200-mb levels, with a peak sensitivity near the 400-mb level. These plumes form a connection that links the Intertropical Convergence Zone (ITCZ) with areas

further north. Such plumes are often associated with the Southwest United States monsoon pattern (Adang and Gall 1989) and are closely tied to flash flood-producing thunderstorms that occur during the monsoon (Fleming and Spayd 1986). That such a tropical moisture plume occurred on the day of the Palomar storm is supported by the analysis sent out over Automation of Field Operations Services (AFOS) provided by the Synoptic Analysis Branch of the National Environmental Satellite, Data and Information Services (NESDIS) on the day of the storm. The AFOS remarks describe the meteorological effects of the deepening central U.S. trough, which has served to force a "dark dry slot south-southwestward into eastern Arizona and New Mexico ...and this in turn has forced a tropical moisture plume southward into Mexico and extending into Southwest Arizona and southern California" (NESDIS 1992). The statement also said that tremendous diffluence aloft was helping to maintain the thunderstorm activity. According to the same statement, satellite precipitation estimates over portions of Imperial County were 2.3 to 2.6 inches for the three-hour period from 00 UTC to 03 UTC. Over San Diego County, satellite estimates were somewhat less, about 1.2 inches in the same three-hour period. It is important to note that this time period is somewhat after the most intense rain observed at Palomar and Laguna.

An examination of the satellite imagery and radar summaries on the day of this storm shows that thunderstorm activity was widespread in southern and southeastern California on August 13. Morning activity began over parts of Riverside and Imperial counties and was evident on radar and satellite by 1630 UTC (930 PDT). This activity showed a slow westward movement with time, and produced some heavy rainfall in the desert (see NESDIS statements in previous paragraph), although the sparsity of stations precludes any real knowledge of how much rain fell from the morning system. The Palomar storm evidently developed quite separately from this system. Mostly clear skies prevailed in the early morning hours over extreme southwestern California, but by around 1800 UTC, the beginning stages in the development of the Palomar storm can be seen on the visible and infrared imagery. Very rapid expansion of cold cloud tops occurs during the two half-hour images, and continued expansion can be seen over the next several hours until about the 2230 UTC image, after which time there is noticeable cooling of cloud tops. The heaviest precipitation occurred during the hours from 2015 to 2115 UTC, when cloud tops appeared to be at their coldest, indicating the period of most intense convection. The rapid expansion of cold cloud tops is one of the key ingredients in the convective -precipitation-estimation technique used by NESDIS (Juying and Scofield 1989). In addition, the Palomar area is

close to the center of the visible anvil, an area where the heaviest precipitation is usually found in storms with weak vertical shear, which, as noted earlier, was the case for this event.

Given the extremely high moisture in place and a very unstable air mass, all that was needed to cause significant convection was a lifting mechanism. The importance of having such a mechanism cannot be understated. For instance, despite the high moisture at San Diego noted earlier, only .05 inches fell that day. Lifted indices in southern California fell from +1 at 00 UTC on August 13 to -4 at 00 UTC on August 14. K-indices were also quite high, 36 for both time periods, a value associated with about an 80 to 90 percent probability of thunderstorm occurrence in the western United States (Lee 1973). The lifting mechanism for the development of this storm is not immediately apparent from an inspection of the synoptic weather maps. There is no organized low pressure area or front traversing the region on August 13. The baroclinic model (Aviation) analysis for 1200 UTC August 13 to 00 UTC August 14 does show a weak (8 unit) vorticity maximum moving from western Arizona to southern California. Such positive vorticity advection is associated with upward vertical motion. This vorticity maximum may in fact be a reflection of a westward-moving tropical wave (often referred to as an *easterly wave*). The possible role of tropical waves in producing extreme rainfall in southern California has not been fully explored, but might provide some interesting findings.

Perhaps the simplest lifting explanation is the orographic effect of the mountains. The highest rainfall amounts at Palomar and Mt. Laguna are centered over the highest local terrain, strongly suggesting that orographic uplift was responsible for producing the critical lift necessary for these extreme thunderstorms. Another possible factor is that outflow boundaries from the morning thunderstorm activity over portions of Riverside and San Bernardino counties helped to initiate new convection further west over and near the mountains east of San Diego.

9.5 Adjustment for Maximum Moisture

9.5.1 Maximum Persisting 3-Hour Dewpoints

As in all previous PMP studies, surface dewpoint temperatures were used as a measure of the moisture available for a particular storm and to estimate the theoretical upper limit to moisture for storms occurring at a specific time and place. The rationale for using surface dewpoints, as opposed to other measures of atmospheric water vapor such as precipitable water or humidity at various levels, has been discussed in several other HMRs. It is easily the most widely available measure of atmospheric moisture in terms of both spatial and temporal coverage. PMP studies have long employed the concept of maximum-persisting dewpoints to provide an upper-limit moisture availability index. The maximum-persisting dewpoint temperature is defined as the maximum dewpoint temperature which is equaled or exceeded at any observation point for the specified period. For a 3-hour period with hourly dewpoints of 70, 71, and 72 °F, the maximum persisting dewpoint would be 70°F; that being the highest reading not undercut at any observation point during the sequence.

HMR 57 was the first study to use 3-hour, instead of 12-hour maximum persisting dewpoints for local-storm analysis. It is hypothesized in that report that the moisture necessary for local storms does not need to be as widespread or persistent as for general storms. Further, it was felt that the duration of the representative dewpoint for a storm should be correlated with the storm duration. Local storms are by definition much shorter in duration than 12 hours, with 3 hours being close to the median for local storms in the western United States Because HMR 49 used 12-hour persisting dewpoints for its local-storm study, it was necessary to develop a new climatology of 3-hour persisting dewpoints for the current study.

Table 9.2 shows the list of surface observation stations used in the development of this new dewpoint climatology, while Figure 9.3 shows the location of these stations. As in the general-storm situation, high dewpoint episodes while rain was falling, or when there was virtually no chance of rain, were not used. An example of a no-rain situation is the existence of an inversion where low-level moisture becomes trapped near the surface, and

Table 9.2. *Surface airway stations for dewpoint climatology.*

Station Name	Latitude	Longitude	Elevation (ft)	Years
Camp Pendleton MCAS	33°18'	-117°21'	76	18
Lemoore Reeves NAS	36°20'	-119°57'	240	27
Long Beach WSCMO	33°49'	-118°09'	25	43
Bakersfield Meadows	35°25'	-119°03'	495	44
Bishop AP	37°22'	-118°22'	4108	44
Daggett FAA AP	34°52'	-116°47'	1922	44
Los Angeles Intl AP	33°56'	-118°24'	97	45
San Diego Lindbergh	32°44'	-117°10'	13	44
Santa Barbara FAA AP	34°26'	-119°50'	9	28
Blue Canyon	39°17'	-120°42'	5280	41
Oakland Metro AP	37°44'	-122°12'	6	36
Sacramento Exec AP	38°31'	-121°30'	18	45
San Francisco Int AP	37°37'	-122°23'	8	44
Stockton Metro AP	37°54'	-121°15'	22	36
Alameda NAS	37°44'	-122°19'	16	43
Crows Landing	37°24'	-121°08'	164	7
Moffett Field NAS	37°25'	-122°03'	39	43
Santa Maria AP	34°54'	-120°27'	254	38
Mount Shasta	41°19'	-122°19'	3590	38
Red Bluff FSS	40°09'	-122°15'	349	39
Redding Mun AP	40°30'	-122°18'	502	6
Arcata AP	40°59'	-124°06'	203	43
El Toro MCAS	33°40'	-117°44'	381	43
China Lake Armitage	35°41'	-117°41'	2220	43
Miramar NAS	32°52'	-117°08'	459	41
Point Mugu NF	34°07'	-119°07'	10	42
San Diego North Isl.	32°42'	-117°12'	49	43
Tustin MCAF	33°42'	-117°50'	59	40
Imperial Beach REAM	32°34'	-117°07'	20	40
San Nicholas Isl.	33°15'	-119°27'	568	42
San Clemente I. NAAS	33°01'	-118°35'	171	28
Twentynine Palms NAAS	34°13'	-116°03'	1765	5
Fresno Air Term.	36°47'	-119°43'	336	44
Yuma, Arizona	32°40'	-114°36'	213	7
Las Vegas, Nevada	36°05'	-115°10'	2162	45
Reno, Nevada	39°30'	-119°47'	4409	43
Medford, Oregon	42°23'	-122°53'	1300	44

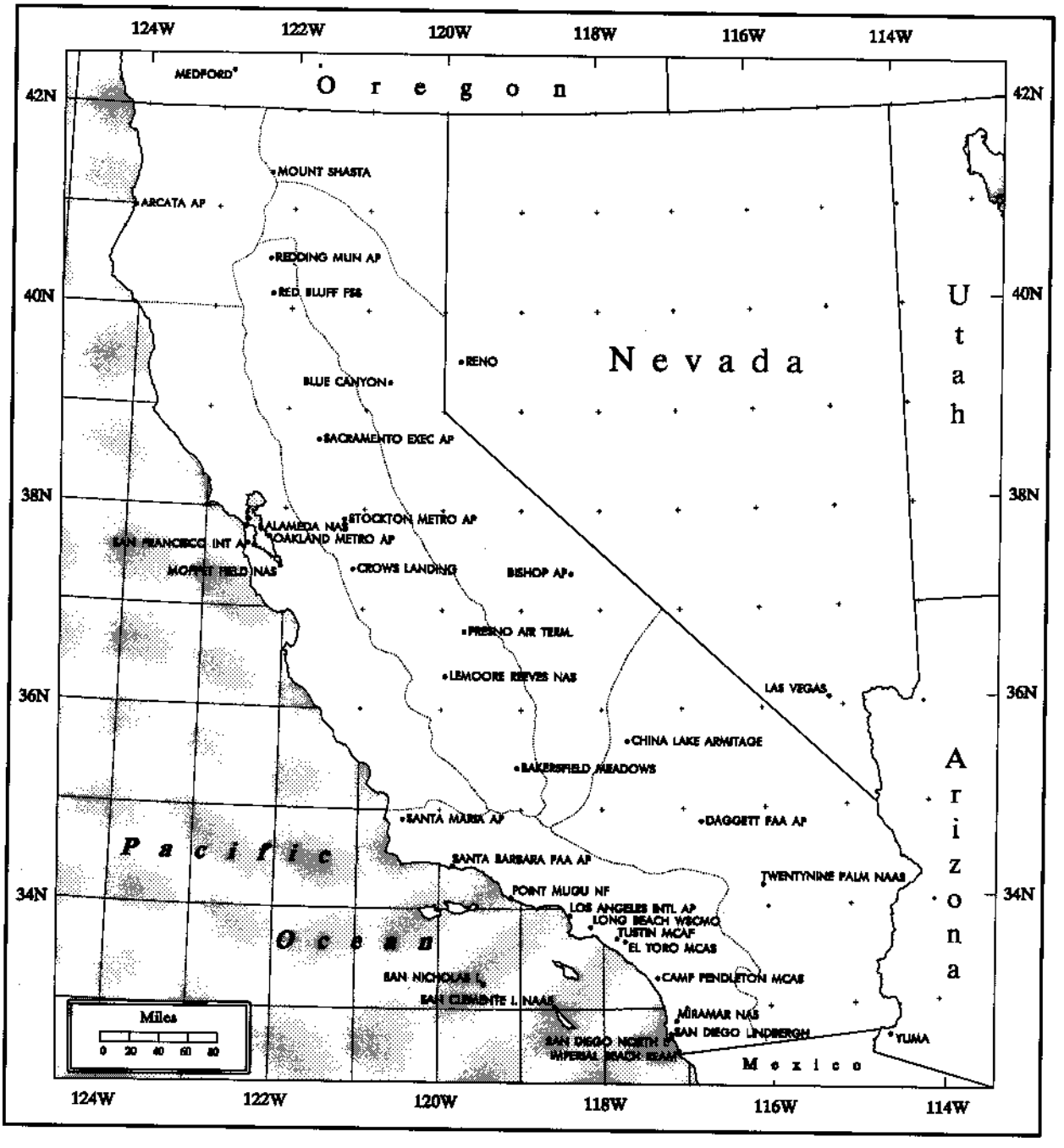

Figure 9.3. *Surface observation stations used in the development of the three hour persisting dewpoint maps (Figures 9.4 to 9.15).*

does not reflect a saturated air mass through the depth of the atmosphere. Such capping of the lower atmosphere is common under calm, anticyclonic conditions. Table 9.2 shows 37 stations in California and adjacent states of Oregon, Nevada and Arizona that were used in the analysis. The period of record was variable, but the majority of stations had at least 30 years of data. The earliest records date from the mid-1940's, while the latest cover through early 1992.

The stations used in the dewpoint analysis ranged in elevation from near sea level to over 5000 feet, requiring that all values be adjusted to a common reference value. As in previous PMP studies, the 1000-mb level was used and all dewpoints were adjusted using a saturated pseudo-adiabatic atmosphere, with data from Technical Paper No. 14 (U.S. Weather Bureau 1951), which provides precipitable water and other moisture-related factors for a saturated pseudo-adiabatic atmosphere. After the data were adjusted to 1000 mb, software was developed that extracted a limited number of the highest dewpoint sequences. The actual number was based on whether or not *good* meteorological sequences could be found, i.e., those not contaminated by rainfall or unusual moisture stratification (admittedly a difficult condition to identify in the absence of nearby atmospheric soundings). Data outliers were checked and discarded if found to be in error or clearly defied the prevailing data pattern. The highest (maximum dewpoints) accepted sequences were then plotted for each station and the general pattern of isodrosotherms (contours of equal dewpoint) drafted. The initial spatial paradigm was based on several previously existing maximum dewpoint climatologies (United States Department of Commerce, 1948, HMR 36) and of course on the data field itself. In addition, the 12-hour dewpoint analysis contained in the present report (see Chapter 4) was compared to the results of the 3-hour analysis, as an additional check on the pattern and magnitude of the final map values. The difference between isodrosotherms at common reference points on the 3- and 12-hour maps varied from as little as 1°F to a maximum of about 5°F, with an average difference of 2 to 3°F.

A comparison of the 3-hour dewpoint maps in the current study with the 3-hour values shown in HMR 57 along the California border do show some minor differences. Interestingly, the isodrosotherms, in this study, are slightly lower than in HMR 57. The reason for this discrepancy is that HMR 57 used no stations in California to extrapolate the

isolines southward across the Oregon border. The use of Arcata and Mount Shasta in the current study, with 43 and 38 years of data, respectively, enabled the spatial pattern to be better defined in the northern California area, resulting in a slight decrease in the maximum-persisting values.

Figures 9.4 to 9.15 show the mid-monthly analysis of 3-hour maximum persisting dewpoints for California. These dewpoints are used to provide upper-limit moisture fields for maximizing local storms. The seasonal progression of these maps reflects the evolution of the large-scale temperature and moisture variations across the country. During the winter months, from December through April, the highest dewpoints occur in southern California along a roughly north-south gradient. The main moisture source during this season for nearly all of California is the Pacific Ocean. The presence of the cool California current along the immediate coast keeps surface dewpoints lower than might be expected at these latitudes. However, under certain flow patterns subtropical Pacific Ocean moisture is drawn into California beneath strong Southwest flow aloft. Meteorologists have at times referred to this as the *pineapple express*, alluding to the source of moisture over the Hawaiian Islands. This pattern is usually responsible for the highest dewpoint episodes. In the winter months, the dewpoint gradient is quite small over the state, especially in January where the difference across the entire state is less than 3°F.

A transitional period in April to May sees a complete reversal of the pattern with the highest dewpoints now coming from the east. One of the reasons for this pattern is the northward movement of the North Pacific subtropical anticyclone to its summer position and the development of the inland thermal low over southwestern United States, combine to create northerly flow along the west coast, causing significant upwelling of cooler ocean water. These waters modify overlying air masses, and reduce their boundary-layer dewpoint temperatures. This pattern becomes more pronounced as the warm season progresses, reaching a maximum in August, when a strong west to east gradient exists and extreme southeastern California reaches a 3-hour maximum persisting value of 79°F. Such very high dewpoints are likely associated with the intrusion of extremely moist air from the Gulf of California. Hales (1972) was among the first to document the northward movement of moisture from the Gulf of California, while Hansen (1975) demonstrated the importance of such moisture to the development of extreme rainfall events in the west. Douglas (1995)

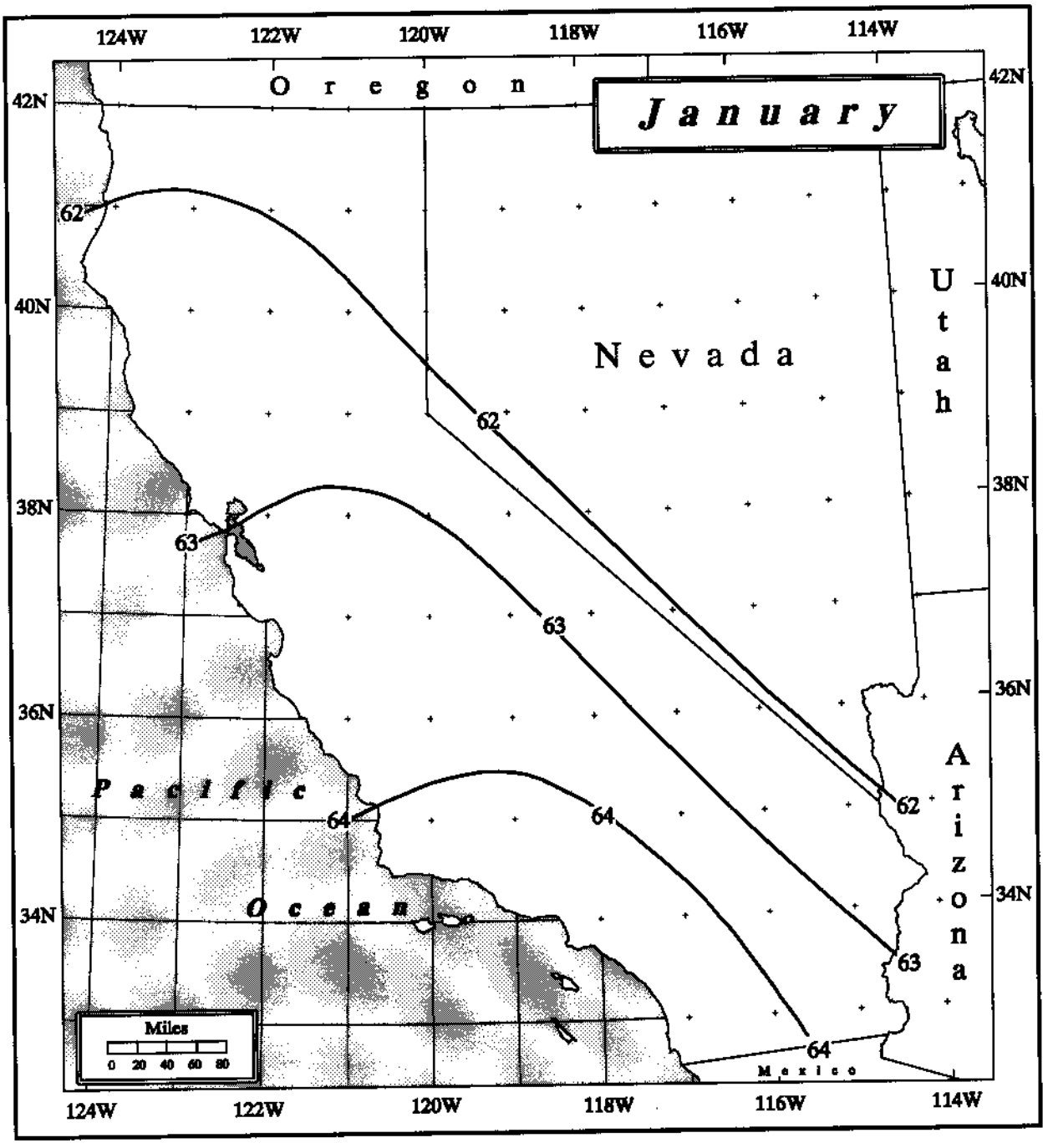

Figure 9.4. *Three-hour maximum persisting 1000-mb local-storm dewpoints for January (°F).*

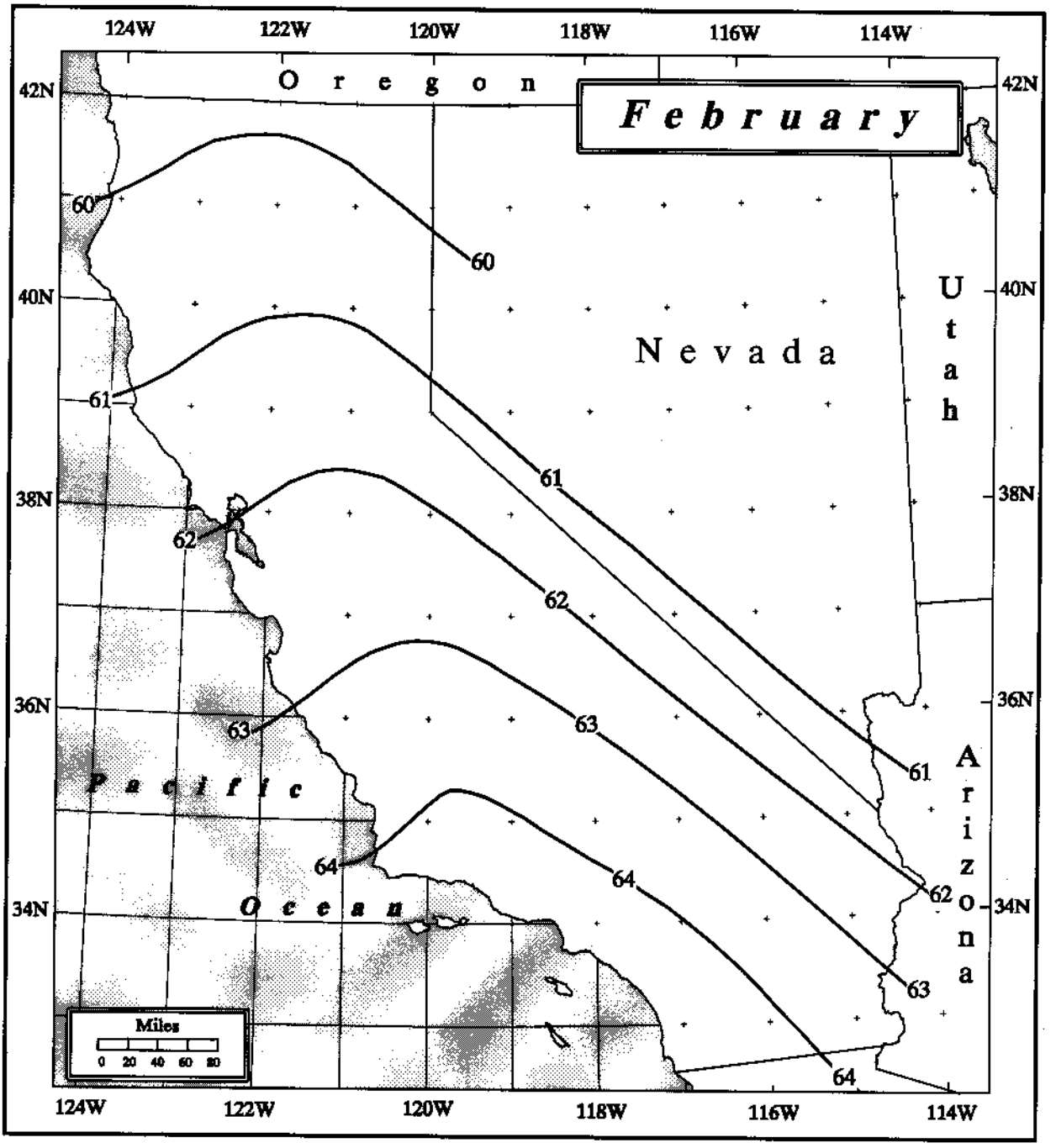

Figure 9.5. *Three-hour maximum persisting 1000-mb local-storm dewpoints for February (°F).*

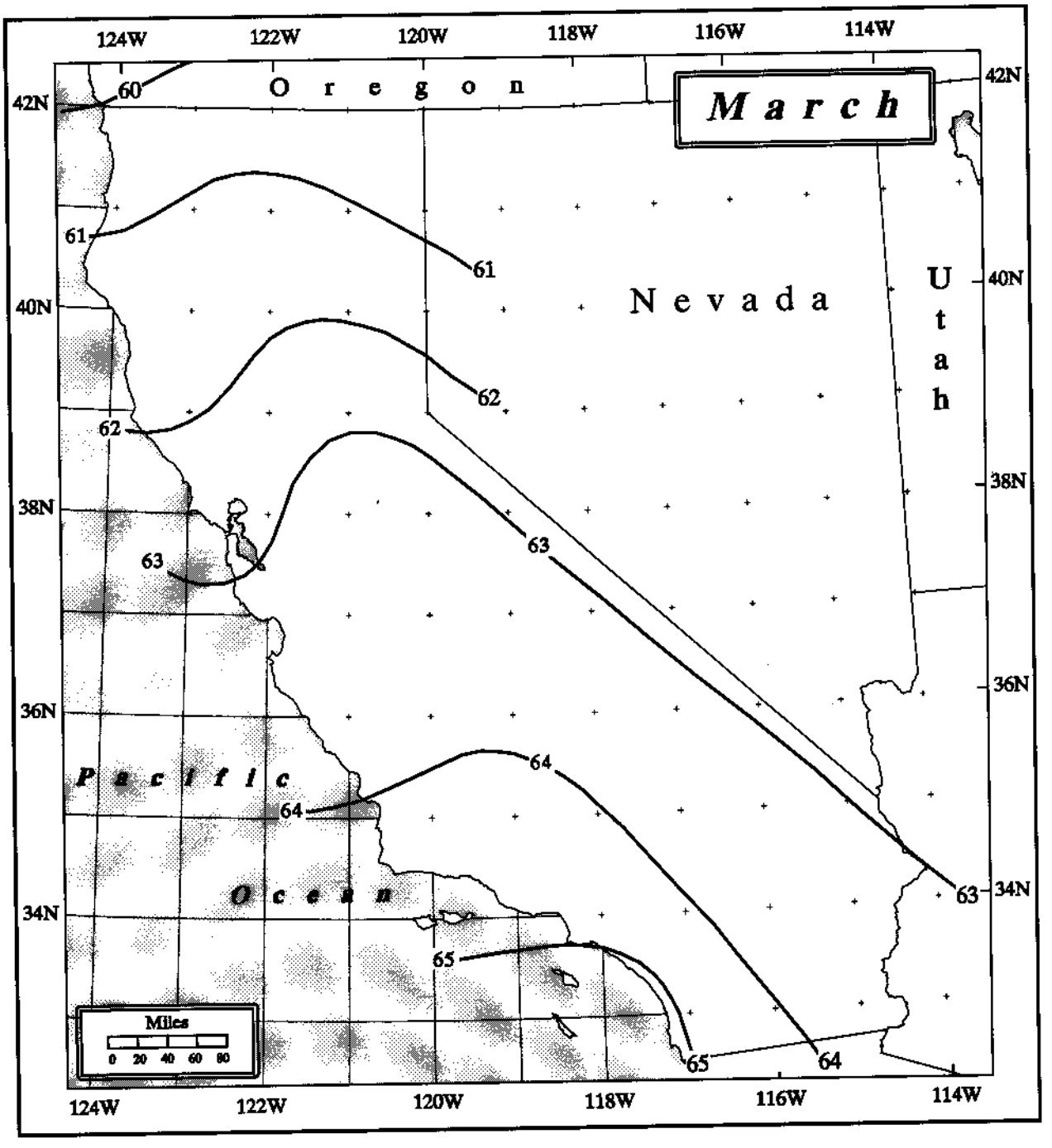

Figure 9.6. *Three-hour maximum persisting 1000-mb local-storm dewpoints for March (°F).*

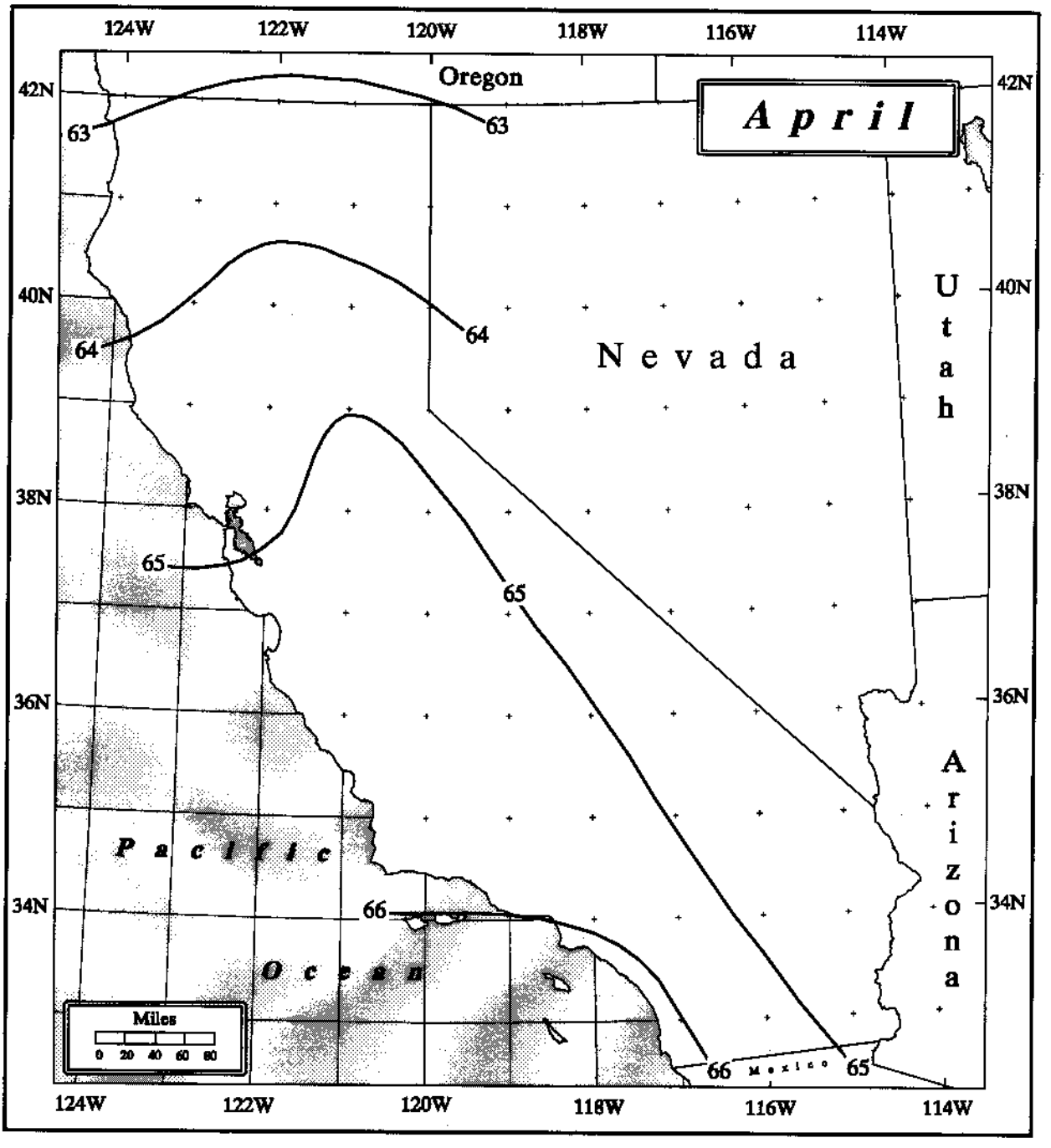

Figure 9.7. *Three-hour maximum persisting 1000-mb local-storm dewpoints for April (°F).*

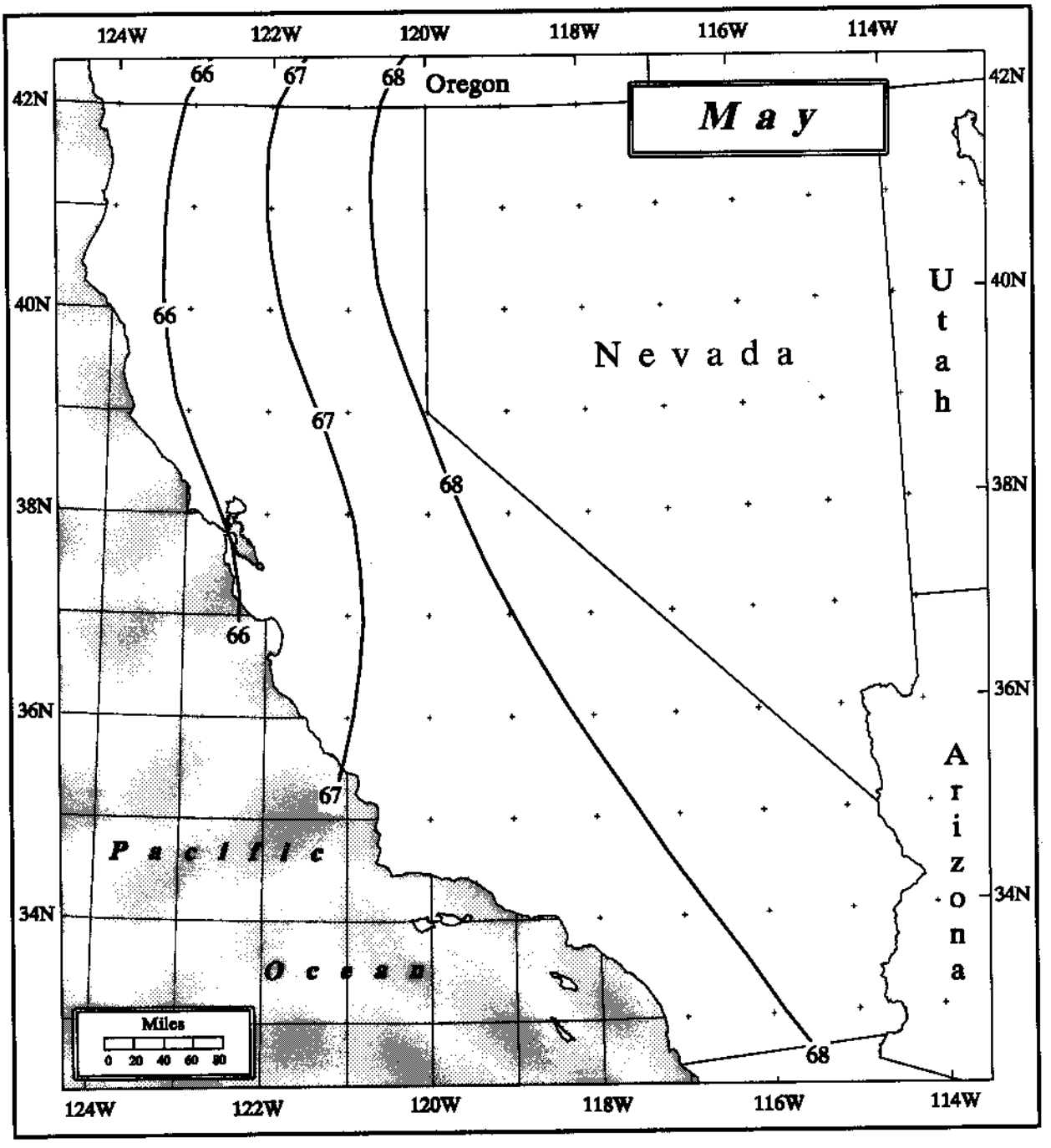

Figure 9.8. *Three-hour maximum persisting 1000-mb local-storm dewpoints for May (°F).*

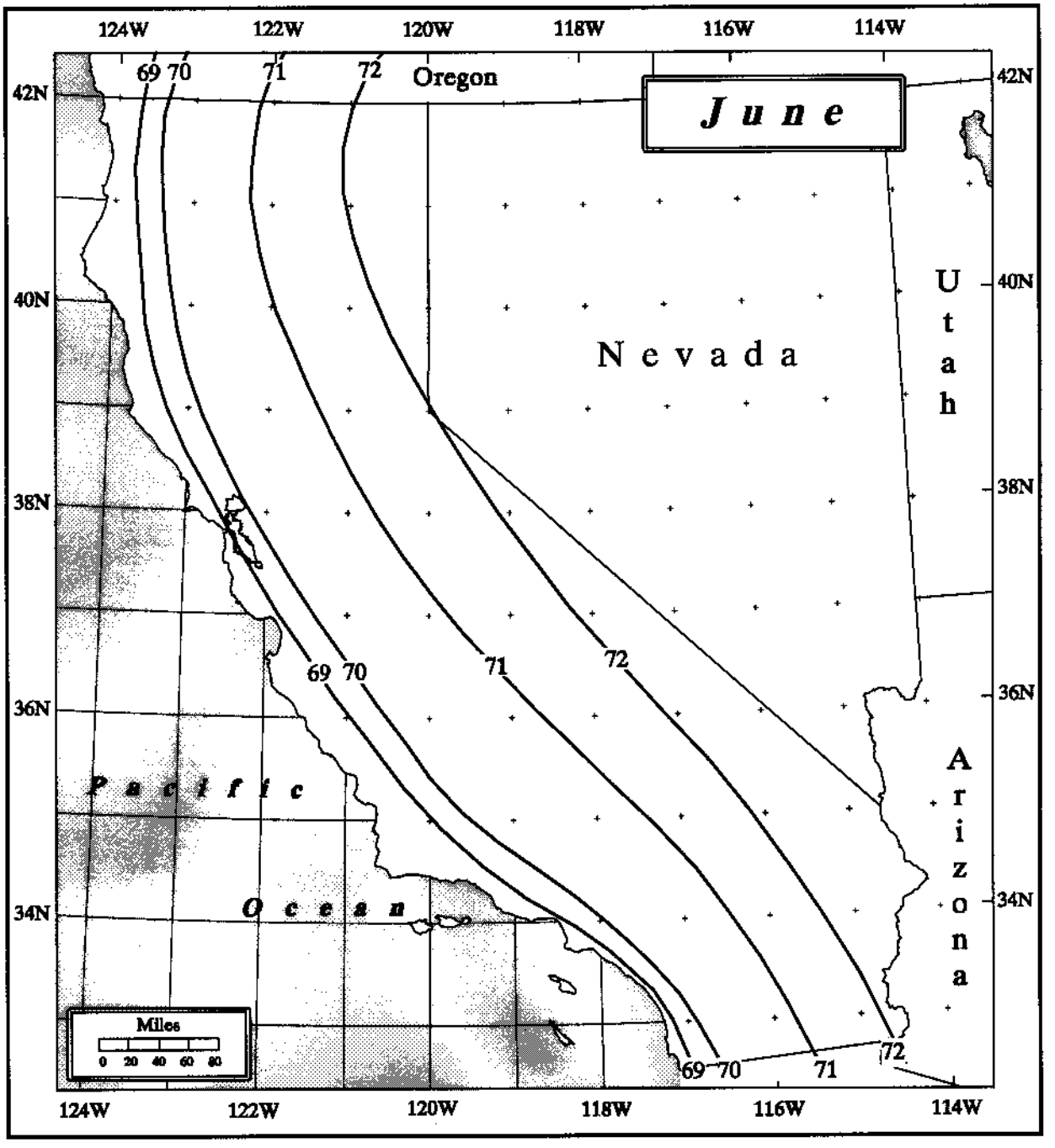

Figure 9.9. *Three-hour maximum persisting 1000-mb local-storm dewpoints for June (°F).*

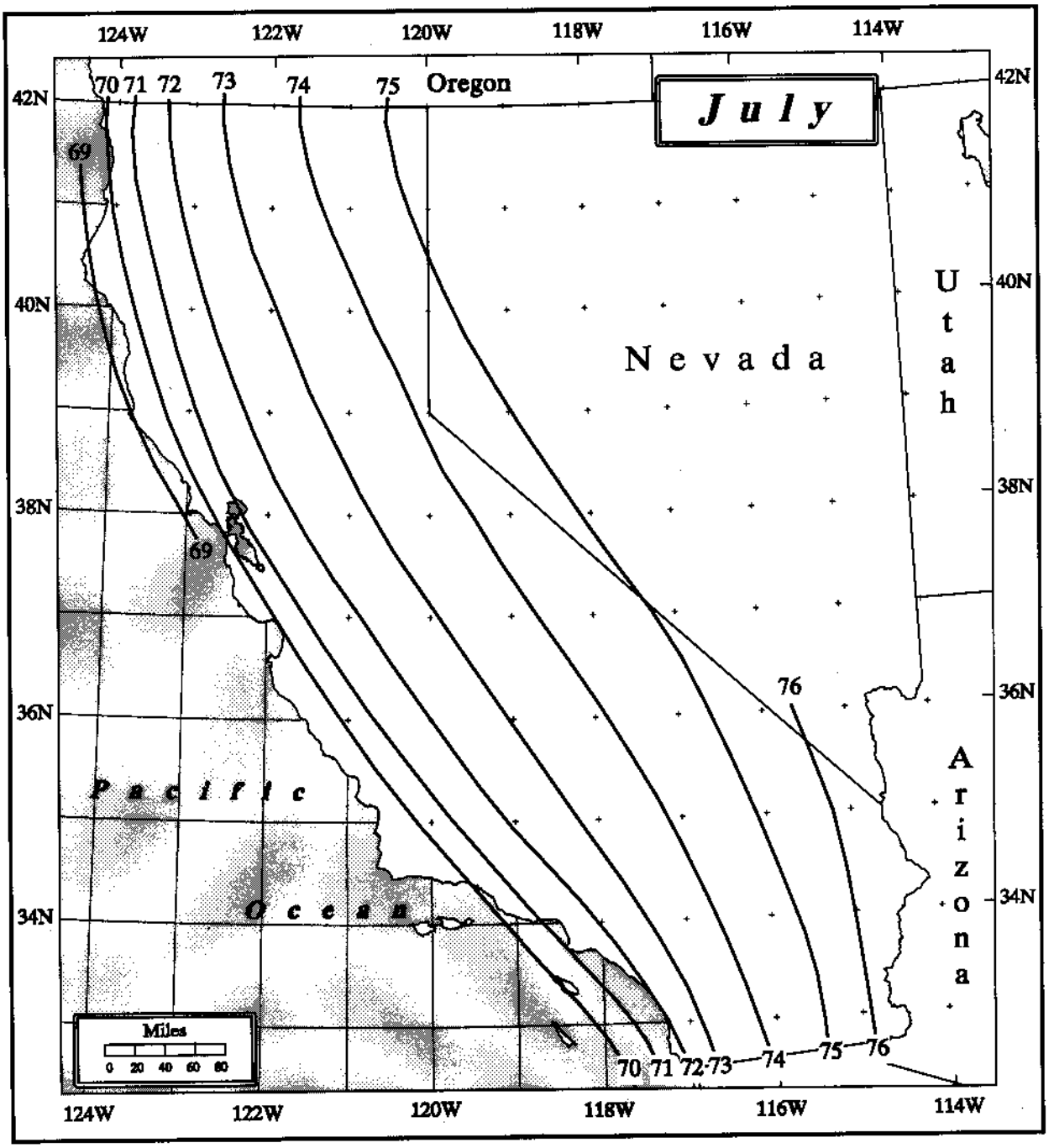

Figure 9.10. *Three-hour maximum persisting 1000-mb local-storm dewpoints for July (°F).*

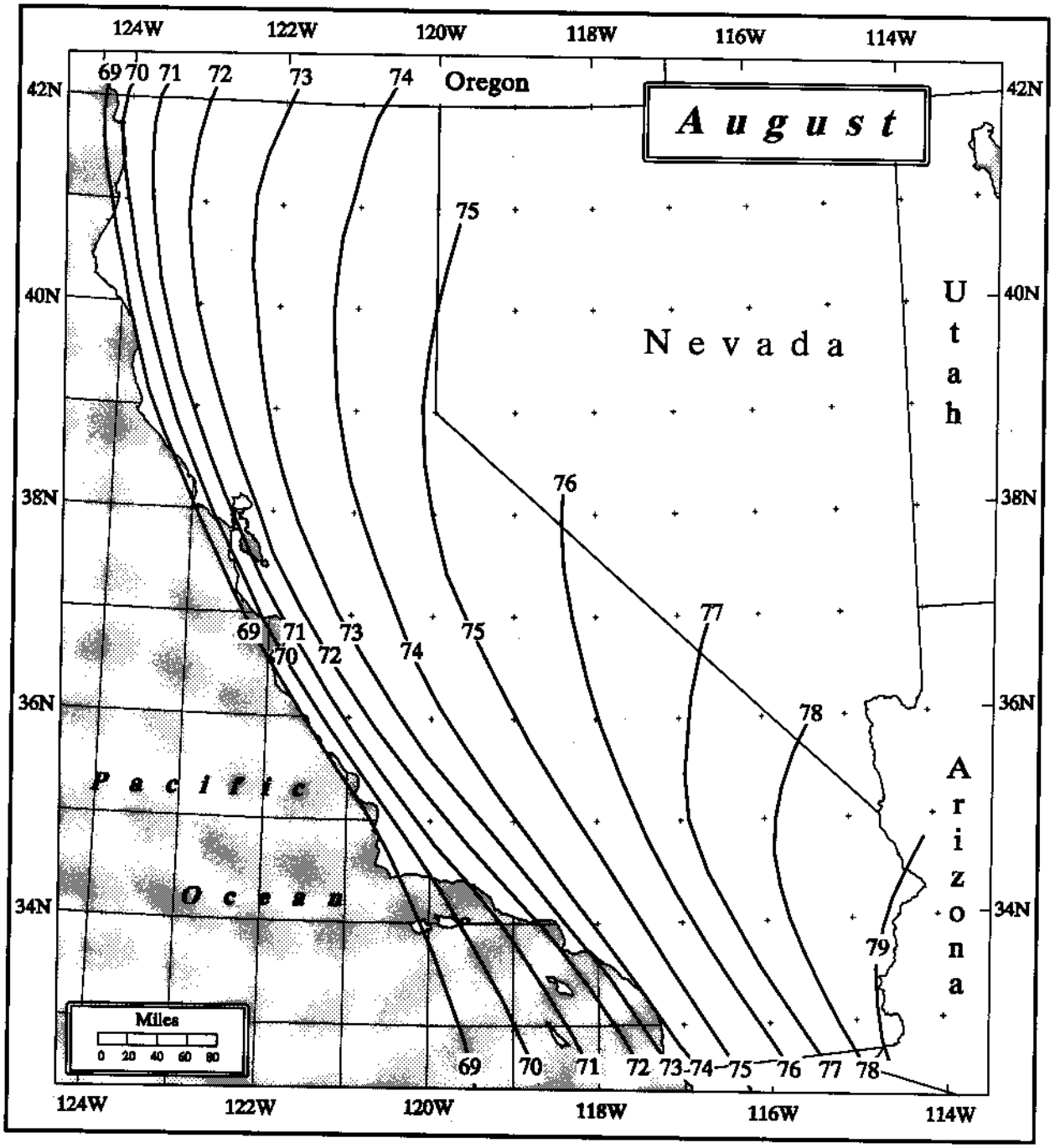

Figure 9.11. *Three-hour maximum persisting 1000-mb local-storm dewpoints for August (°F).*

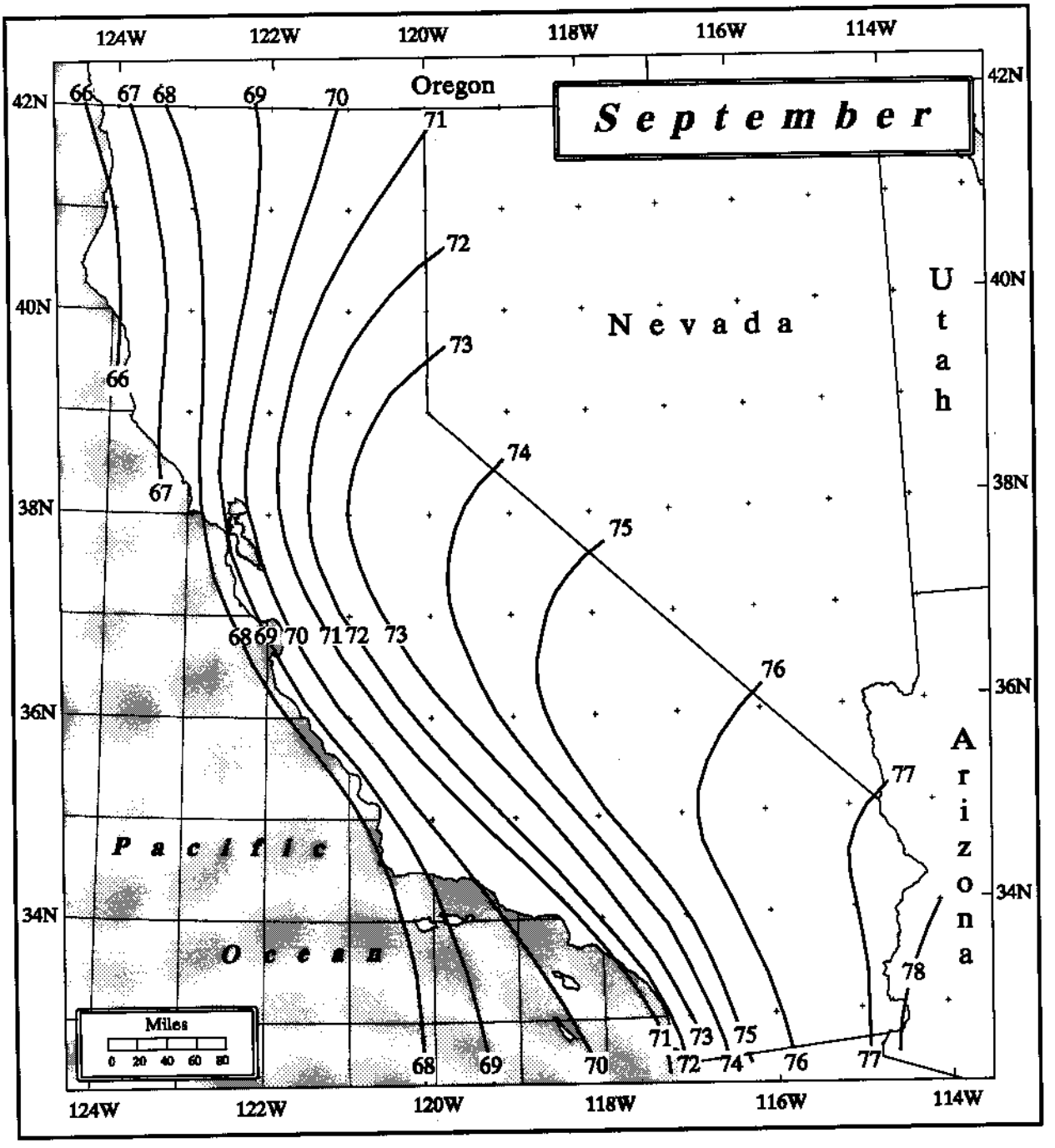

Figure 9.12. *Three-hour maximum persisting 1000-mb local-storm dewpoints for September (°F).*

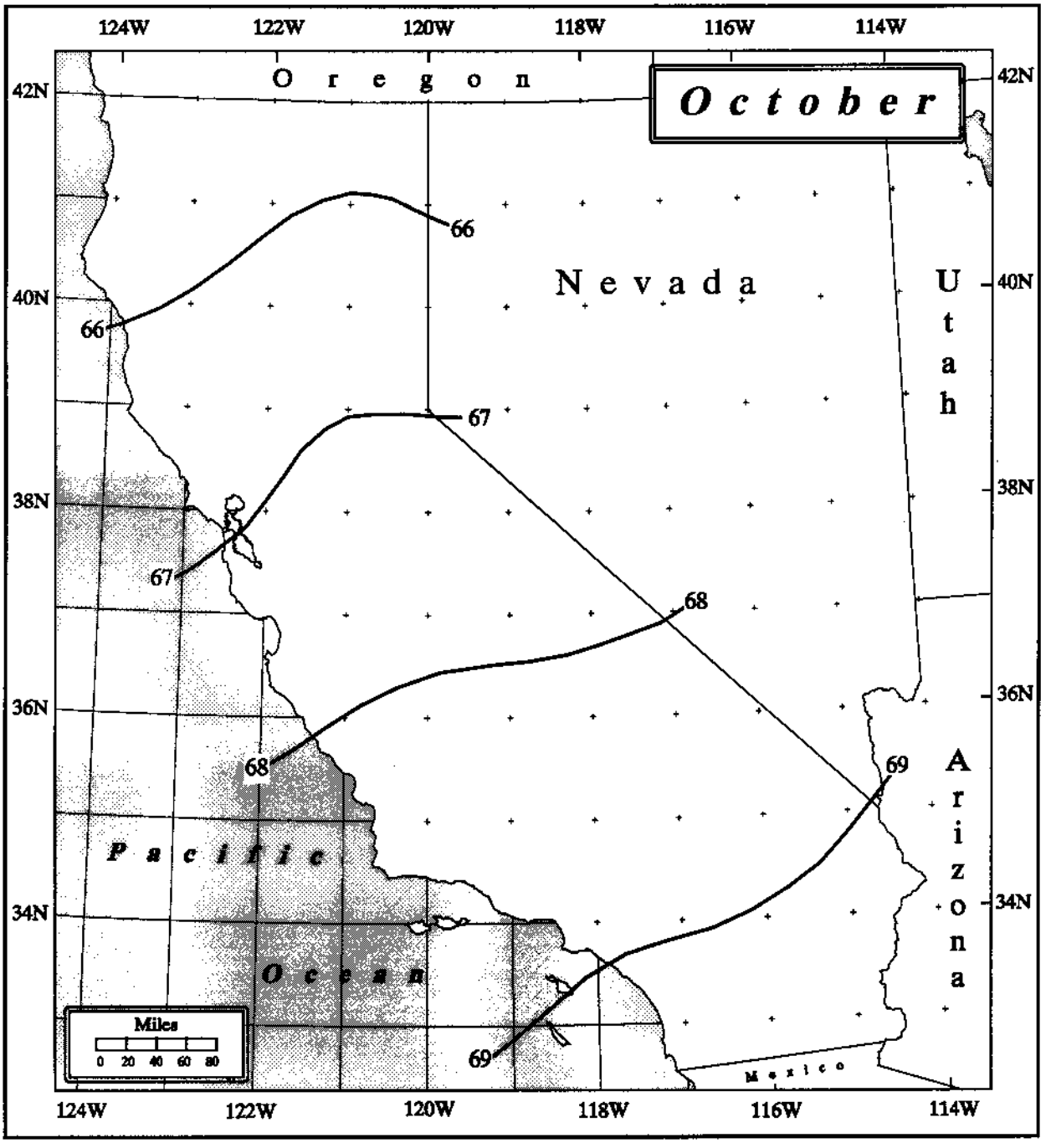

Figure 9.13. *Three-hour maximum persisting 1000-mb local-storm dewpoints for October (°F).*

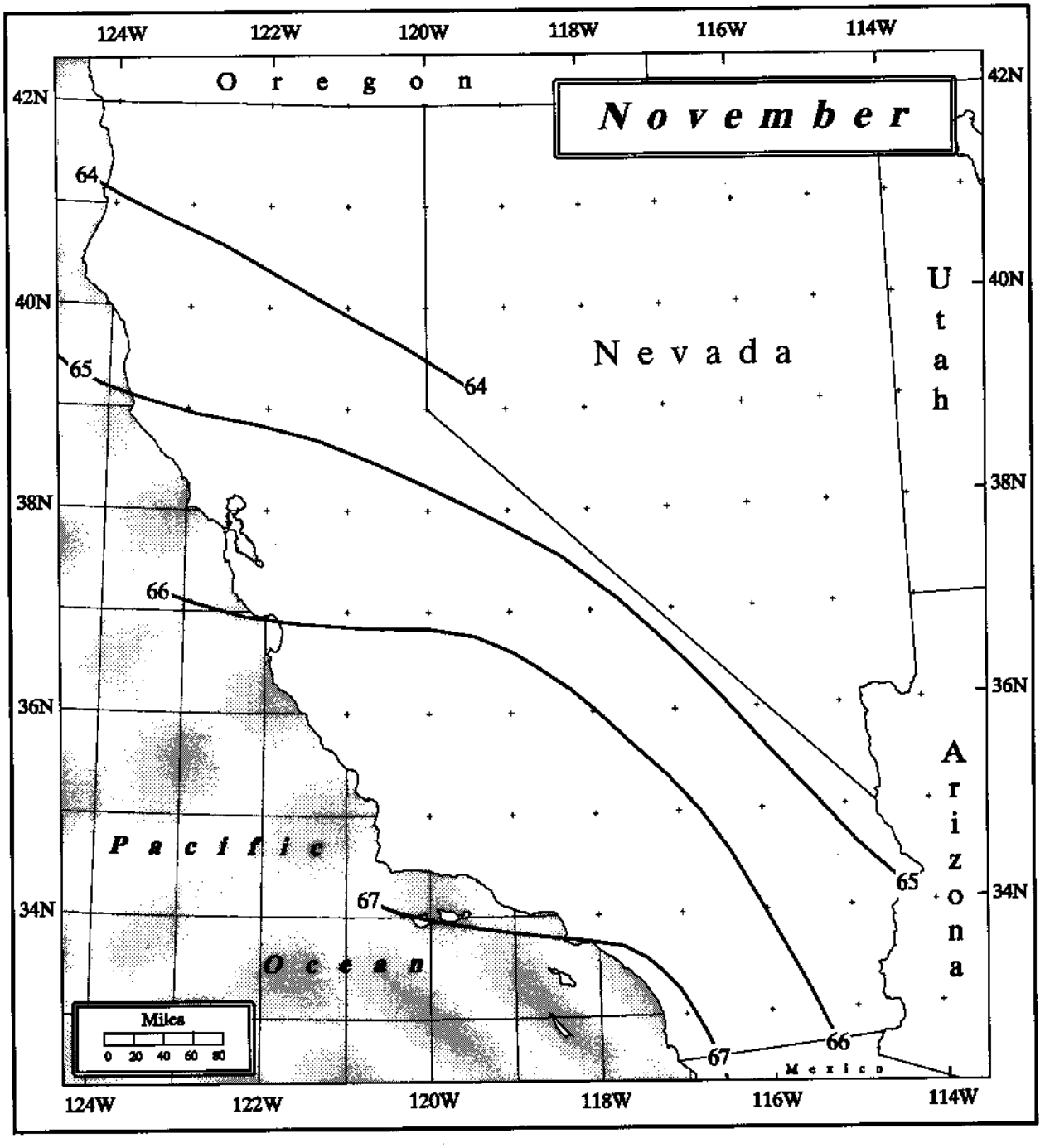

Figure 9.14. *Three-hour maximum persisting 1000-mb local-storm dewpoints for November (°F).*

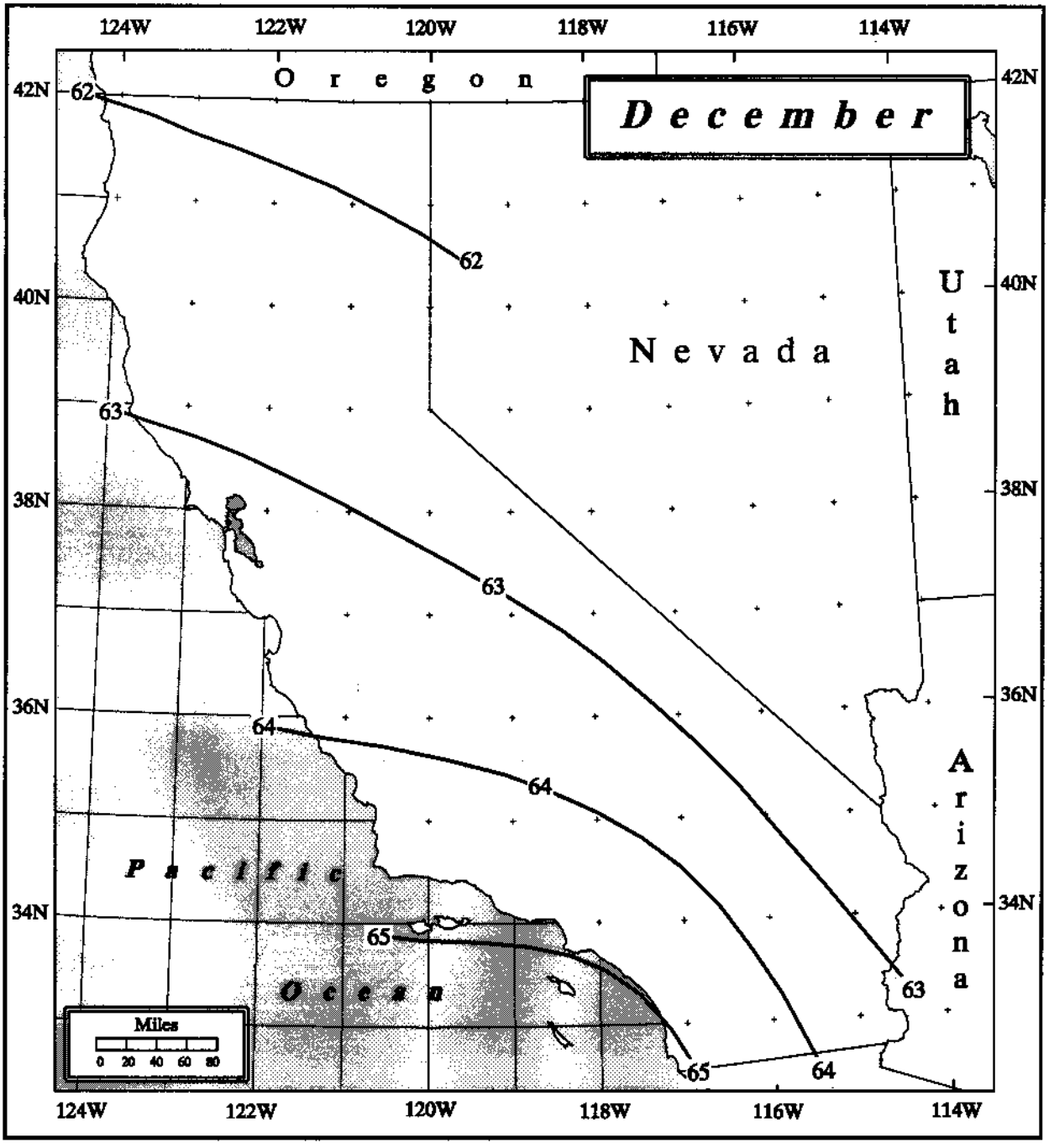

Figure 9.15. *Three-hour maximum persisting 1000-mb local-storm dewpoints for December (°F).*

has confirmed in very recent research the existence of a low-level jet at around 300 meters in the southerly flow over the Gulf of California and adjacent areas. The low-level jet is found to occur under different synoptic flow regimes and is certainly responsible for transporting some of the highest dewpoint air into southeastern California. These low-level intrusions of extremely moist air are probably responsible for the most extreme thunderstorm activity in the deserts of southeastern California. Another very recent study of a severe MCS in central Arizona (McCollum et al. 1995) confirmed that the low-level moisture responsible for the destabilization of the air mass had its roots in the southerly low-level flow from the Gulf of California.

Several studies have detailed the importance of the Southwest monsoon pattern to summertime rainfall over the southwestern United States, mainly during July and August (Carleton 1985, 1986). This pattern, which brings moisture into the Southwest from a westward expansion of the Bermuda High, is also responsible for the advection of significant moisture into California, but most of this moisture is transported in the southeasterly flow at midlevels, from about 700 mb and higher (Watson et al. 1994). It appears, however, that the highest dewpoints are probably associated with the Gulf of California low-level jet. The general pattern with the highest dewpoints over southeastern California with decreasing dewpoints to the northwest, maintains itself during September; but by late October and November, the cool season pattern has reasserted itself, and dewpoints again decrease from west to east.

9.5.2 Adjustment for In-Place Maximization

The in-place adjustment for moisture maximization of local storms is similar to the process for general storms, with some important differences. The adjustment is in the ratio of the precipitable water for the 3-hour maximum persisting dewpoint at the storm location (Figures 9.4 to 9.15) to that for the 3-hour maximum persisting dewpoint for the storm in question. It has been the practice since HMR 55A for the local-storm adjustment procedure not to indicate a specific inflow direction to obtain the storm dewpoint, as is done in general storms. In local storms, the inflow can be specified in any direction from the storm location, because of the assumption that local storms can develop independently of large-scale moisture inflows which sustain extreme general storms. The much smaller scale of local storms in fact makes this practice a necessity, due to the paucity of observations near the